

ÄSPÖLABORATORIET

**INTERNATIONAL
COOPERATION
REPORT**

94-16

**Hydrodynamic modelling of the
original steady state and LPT2
experiments**

MARTHE and SESAME codes

Y Barthelemy, J Schwartz, K Sebti
ANTEA

December 1994

Supported by ANDRA, France

**SVENSK KÄRNBRÄNSLEHANTERING AB
SWEDISH NUCLEAR FUEL AND WASTE MANAGEMENT CO**

BOX 5864 S-102 40 STOCKHOLM

TEL. +46-8-665 28 00 TELEX 13108 SKB TELEFAX +46-8-661 57 19

9506120154
PDR WASTE
WM-11

950602
PDR

112.8

see info on 9506120143 950602

**HYDRODYNAMIC MODELLING OF
THE ORIGINAL STEADY STATE AND
LPT2 EXPERIMENTS**

MARTHE AND SESAME CODES

Y Barthelemy, J Schwartz, K Sebti

ANTEA

December 1994

Supported by ANDRA, France

This document concerns a study which was conducted within an Äspö HRL joint project. The conclusions and viewpoints expressed are those of the author(s) and do not necessarily coincide with those of the client(s). The supporting organization has reviewed the document according to their documentation procedure.

**HYDRODYNAMIC MODELLING OF
THE ORIGINAL STEADY STATE AND
LPT2 EXPERIMENTS
(pumping tests and tracer tests)**

MARTHE AND SESAME CODES

**Y. BARTHELEMY, J. SCHWARTZ, K. SEBTI
ANTEA**

December 1994

Supported by ANDRA, France

ABSTRACT

The modelling of natural and forced hydrodynamic behaviour of Äspö site has been performed with a finite differences code, MARTHE, taking into account the flow in the porous matrix and in 22 large individualized fractures.

Due to many uncertainties on hydrodynamic and geometric parameters, a true calibration of the model was not actually performed, but sensitivity tests have been achieved in order to assess the robustness and accuracy of the conceptual model. This one is judged as a pretty good compromise, even if some hydraulic discrepancies exist, probably caused by some missing fractures such as EW-X.

The transport simulations performed with SESAME, using a Random Walk particle tracking method, gave rather good results for Uranine and Rhenium-186 tracer tests. The differences between observed and simulated breakthrough curves, especially in NNW-1 fracture, could be once again in relation with a missing fracture such as EW-X.

TABLE OF CONTENTS

	Page
SUMMARY	iii
1 INTRODUCTION	1
2 ÄSPÖ ISLAND, SITE OF THE FUTURE HARD ROCK LABORATORY	4
2.1 MAIN STUDIES CARRIED OUT	4
2.2 HYDROGEOLOGICAL PARAMETERS	4
2.3 SALINITY DISTRIBUTION	4
3 CONCEPTUAL HYDROGEOLOGICAL MODEL OF ÄSPÖ ISLAND	6
4. DEVELOPMENT OF THE NUMERICAL MODEL OF ÄSPÖ	10
4.1 AREAL EXTENT OF THE ZONE MODELLED	10
4.2 THE GRID	10
4.3 DISTRIBUTION OF EXCHANGE COEFFICIENTS BETWEEN CELLS	10
4.4 BOUNDARY CONDITIONS	10
4.4.1 Lower Boundary	12
4.4.2 Lateral Boundaries and Upper Boundary (except for the Island)	12
4.4.3 Upper boundary (Island of Äspö)	12
5. MODELLING STEADY STATE CONDITIONS	14
5.1 NUMERICAL METHODS ADOPTED	14
5.2 SIMULATIONS	14
5.3 CONCLUSIONS OF THE STEADY STATE STAGE	19
6. MODELLING TRANSIENT CONDITIONS. SIMULATION OF PUMPING TEST LPT2	20
6.1 LPT2 PUMPING TEST	20
6.2 ASSUMPTIONS FOR MODEL CALCULATIONS	20
6.3 RESULTS	22
6.4 VERIFICATION AGAINST THE DATA OF THE PUMPING TEST LPT1	24
6.5 CONCLUSIONS ON FLOW MODELLING	24
7. MODELLING OF TRACER EXPERIMENTS	28
7.1 EXPERIMENTAL CONDITIONS	28
7.2 MODELLING OF THE TRACER TESTS	29
7.2.1 Numerical options selected for this simulation	29
7.2.2 Modelling of flow paths	31
7.2.2 Modelling of Rhenium	31

7.2.3	Modelling of Uranine	31
7.3	CONCLUSIONS OF THE TRACER TESTS SIMULATIONS	33
8.	GENERAL CONCLUSIONS	35
	APPENDIX - MODELS AND CODES SPECIFICATIONS	36

EXTENSIVE SUMMARY

The BRGM contribution to ANDRA Task Force on Äspö site modelling was divided into three projects, all with the same objective: modelling of natural and forced hydrodynamic behaviour, plus tracers tests achieved during the LPT2 experiment. Those three projects differed by the codes they used:

- a finite difference (F.D.) code MARTHE, used for hydraulic simulations, and a hydrodispersive model SESAME for transport computations by a particle tracking method;
- a discrete stochastic code CHANNET (Channel Network), taking into account the fracture porosity only, for both hydraulic and transport simulation;
- a finite element (F.E.) dual porosity code ROCKFLOW, for both hydraulic and transport simulations.

The present report is dedicated to the first project, with the MARTHE and SESAME codes. The F.D. method offers the interest of an easy and quick gridding with parallelepipedic cells, but with the disadvantage of imposing the same shape to all the cells, which does not allow a really good adequacy between the grid and the geometry of the fracture medium.

This main disadvantage is greatly reduced with the introduction of an algorithm previously developed by Urban SVENSSON. This one consists in determining, by means of a geometric calculation, the intersections of fractures with the faces of each cell, then calculating the exchange coefficients between the cells, resulting from the superimposing of fracture transmissivities over matrix permeabilities. Calculation of the intersections of each fracture with each cell boundaries allows a precise evaluation of the exchange coefficients through the six boundaries of each cell of the model grid, taking into account the real dip of the fractures. In this way, it was possible to create a grid of 19,488 parallelepipedic cells, corresponding to a 1,800 x 1,800 m x 1,235 m volume, in which the 22 fractures planes of the SKB conceptual model were taken into account.

In the absence of information on fractures extensions, some hypotheses were made on these data, detailed in the report. Transmissivities of fractures were chosen very close to the SKB values, while uniform permeability of 10^{-8} m/s was assigned to the whole matrix. Densities and heads were imposed on lateral boundaries as functions of depth under sea level.

By computing both pressure and salt concentration fields by iterative resolution of coupled flow and transport equations, it was possible to model the natural conditions supposed to represent the hydraulic steady state. For the infiltration rate on the Äspö island it was necessary, in order to recover a piezometry close to the

observed levels, to retain a much lower rate than the recharge estimated from hydroclimatic calculations (5.5 mm/year instead of more than 120 mm/y). This discrepancy had already been mentioned by U. SVENSSON who found with the PHOENICS code a recharge value of 3 mm/year.

Except for this point, the results obtained were rather satisfactory: the natural piezometric state was reproduced with a good accuracy, while sensitivity tests brought into light the importance of different parameters such as the matrix conductivity, the water salinity variation with depth, the transmissivities of the fractures and the infiltration rate.

For the LPT2 pumping test simulations, the inflow distribution, measured during spinner test, was distributed amongst the four conductive faults which intersect KAS06. A uniform specific storage coefficient was assigned both for matrix and fractures, in addition with a free storage coefficient in unconfined zones.

An analysis of the sensitivity of the calibration parameters revealed the following:

- very little changes of the density field during the pumping test,
- specific storage coefficient between $5 \cdot 10^{-7} \text{ m}^{-1}$ and $5 \cdot 10^{-8} \text{ m}^{-1}$.
- free storage coefficient range from 2% to 5%,
- need to extend the lateral boundaries of the model,
- need to decrease the vertical transmissivity at sea bottom, assuming a fracture clogging by sea deposits.

A rather good agreement between measured and simulated drawdowns was obtained, in particular in fractures EW-3, EW-5, NNW-2 and NE-2, while a substantial under-estimation of drawdowns was simulated in fracture NNW-1.

Globally, it appears that the SKB conceptual model is a good compromise, and modelling it with MARTHE yields reasonable fit to the measures, with parameters close to those of SKB's model.

The transport simulations were performed with SESAME, using a Random Walk particle tracking method, computing the velocities from the fluxes calculated by MARTHE with the hypothesis of a single porosity model.

The six tracer experiments were simulated, and the model was calibrated on the breakthrough curves of Uranine and Rhenium-186, the both tracers detected in the pumping borehole KAS06. The tracer tests were modelled as series of pulses injected in various boreholes sections, taking into account the recovery rates (28% and 30% respectively).

The results obtained are good in fractures NNW-2 and EW-5, but there is a problem regarding the intersection of KAS06 with the fracture NNW-1, where simulations give almost no tracer while measures show effective breakthrough

curves. This might confirm an indication of a local problem on connection between fractures, as for the transient state modelling. One or several EW-X fractures added in the conceptual model should increase hydraulic connections, and possibly improve the tracer simulations concerning NNW-1.

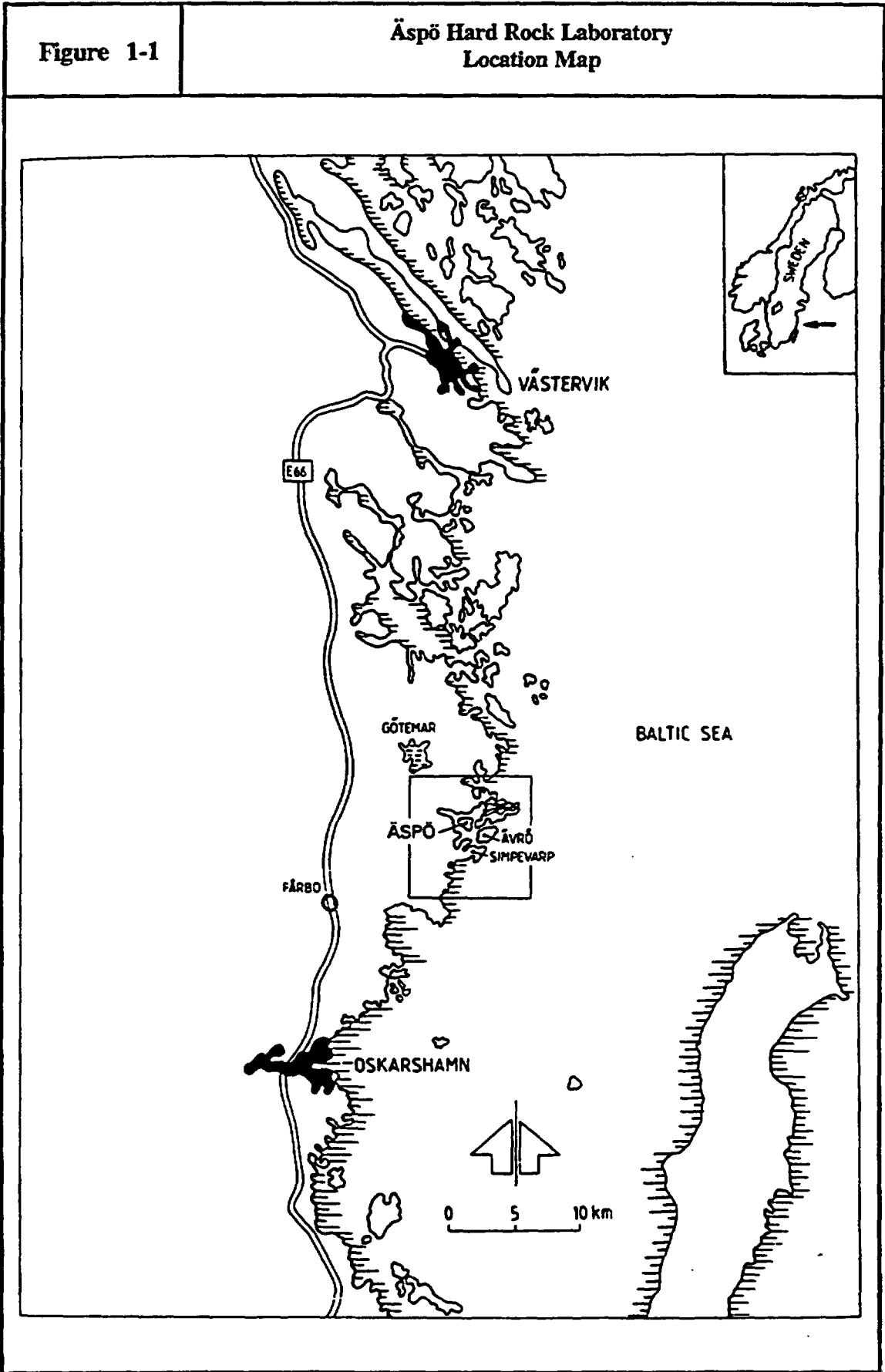
It can be noticed that there is a good coherence of the hydrodispersive parameters deduced from the Uranine and Rhenium-186 tracer tests: $\alpha_L = 20$ m, $\alpha_T = 1$ to 3 m, $\omega = 9.10^{-5}$ to 30.10^{-5} . Hypotheses can be proposed to explain the rather low recovery rates.

INTRODUCTION

ANDRA (Agence Nationale pour la gestion des Déchets Radioactifs) is in charge of the French Nuclear Waste Disposal Programme: low activity and short lived wastes in surface repositories, and high activity wastes in deep geological formations. Several possible sites have been investigated in France as candidates for underground laboratories and eventually future disposal location. Early 1990, the French Government has decided a moratorium to this programme, leaving time to further technical and scientific evaluations, as well as public inquiries. Since then, field works and in situ investigations have been halted on the French territory. In the meanwhile ANDRA has turned its technical activity towards general methodology and to participation to field studies in foreign countries: principally, Belgium (Mol site), Canada (the AECL'S Underground Research Laboratory) and Sweden (the Hard Rock Laboratory of Äspö).

The island of Äspö is a granitic coastal island in the Baltic sea [Fig. 1-1], separated from the Swedish main land and several other islands by shallow arms of sea, no larger than a few hectometers. Its context is considered as representative of a possible deep repository site in granite; so the Swedish organisation for Nuclear Waste Disposal, SKB (Svensk Kärnbränslehantering) has been asked to design, build and operate an underground laboratory, at a depth of 500 m, accessible by a gallery. The aim of this facility is to assess, by experiments of various types, the safety of an eventual repository in such a formation. This decision has been taken after extensive investigations on the site, from 1986 to 1990: geology, geophysics, hydrology, geochemistry... In particular, it yielded knowledge over the geometry and the hydraulic conductivity of the granite formation and its system of fractures, studied from the surface and in boreholes where hydraulic conductors were isolated between packers. The investigations on groundwater flow and transport have been interpreted by various conceptual and mathematical models, implemented by several teams: particularly, flow under the natural initial conditions, and flow in the context of two long-duration pumping tests (LPT1 and LPT2), as well as tracer tests performed during LPT2. Finally SKB has chosen a model by U.Svensson, using the code PHOENICS, to predict the hydraulic impact of the future Hard Rock Laboratory (HRL).

The construction of this facility started in October 1990 by the excavation of a gallery that should reach the level -500 m by 1994. This gallery is under constant monitoring; it is periodically the object of comparisons between model-predictions and observations, while these observations allow conceptual model updating. SKB has organized a forum of 12 organizations from various countries supporting the Äspö HRL, under the name of Äspö Task Force. Its aim is to interact in the area of conceptual and numerical modelling of groundwater flow and solute transport in the Äspö fractured rock. The Task Force interacts with the principal investigators responsible for carrying out experimental and modelling work at the Project. In particular, it participates to the conception of the future experiments (equipment and



operation). As a preliminary step, the Task Force members have worked on the modelling of the original steady state of the groundwater, and the long duration pumping tests and tracer experiments. Their methodologies, hypotheses and results are to be compared together and with the original model by U.Svensson.

ANDRA is a member of the Äspö Task Force, with L.Dewière as its representant. In order to fulfill this preliminary step, ANDRA has contracted three organizations (BRGM, C.E.A. and ITASCA International) who performed the modelling with distinct approaches:

- C.E.A. by a finite element code (TRIO),
- BRGM and ITASCA jointly, by a discrete fracture model (code CHANNET),
- BRGM by two distinct approaches: (i) flow by finite differences and transport by particle tracking (code system MARTHE-SESAME), and (ii) flow and transport by a finite element code (ROCKFLOW).

The present report concerns the MARTHE-SESAME approach, where flow accounts for density distribution and double porosity effect (a conductive set of fractures intersecting a permeable rock matrix). MARTHE performs the calculation of heads, fluxes and density distribution by a finite difference method; SESAME, computes transport by a Random Walk particle tracking method. The model was calibrated against the natural steady state, then it was applied to the long pumping tests LPT2, and LPT1. The fluxes computed by MARTHE served as input for SESAME in the simulation of the LPT2 tracer tests.

ÄSPÖ ISLAND, SITE OF THE FUTURE HARD ROCK LABORATORY

Located 300 km South of Stockholm, Äspö Island is the site for the future underground laboratory to be built at a depth of 500 m. This laboratory, named HRL for Hard Rock Laboratory, will be linked to the surface both by a partly helicoidal gallery and by a vertical shaft. Excavation work began in 1990 and should be completed in 1994. In early 1993 a depth of 300 m had been reached.

2.1 MAIN STUDIES CARRIED OUT

Many studies have been done on the site since 1986 in order to determine its mechanical, hydraulic and chemical characteristics. Äspö Island is made up of poorly permeable granitic formations intersected by large hydraulically conductive fracture zones. These formations continue under the Baltic Sea and outcrop on the coast and the neighbouring islands. All of the site is saturated with water whose salinity increases with depth.

2.2 HYDROGEOLOGICAL PARAMETERS

The various studies carried out have shown that:

- The conductivity measured in the rock matrix ranges from 10^{-11} to 10^{-5} m/s. There is no clear correlation between the measured permeabilities and the geographic or lithological zones nor the depth. They follow a log-normal distribution with an average value around 10^{-8} m/s.
- No information is available on the storage coefficient of the rock matrix.
- The transmissivities of the main fracture zones range from $5 \cdot 10^{-7}$ to $4 \cdot 10^{-4}$ m²/s, with most of the values between 10^{-5} and 10^{-4} m²/s. Their widths range from 1 m to 100 m.
- The specific storage coefficients are estimated to be between 10^{-8} and 10^{-6} m⁻¹.

2.3 SALINITY DISTRIBUTION

The salinity measured in the wells shows that fresh water from rainfall does not reach depths below several tens of meters. Only one well encountered freshwater at 40 meters.

It seems that fractured zones play an important role in the distribution of salinity by favouring, at the same time, the infiltration of fresh water and the rise of deep saltwater.

In order to take into account values measured both in the wells and in the Baltic Sea, the equation selected by SKB for the distribution of salinity S (in g/l) as a function of depth z (m) is $S = 7 + 0.012 z$ (Rhen, 1990, Appendix B3).

CONCEPTUAL HYDROGEOLOGICAL MODEL OF ÄSPÖ ISLAND

The conceptual model developed by SKB can be described by the following simple characteristics:

- In an early step, the granitic matrix was divided into several zones called GPAs (GPA = General Properties Area), with different permeabilities deduced from pumping test. But finally, the role of this distinction was not evident as fractures appeared to play a preponderant role. As a first approach, we considered the rock to have a homogeneous permeability of 10^{-8} m/s, the average value measured on site.
- The existence of 22 conductive fractures whose transmissivities were deduced from the interpretation of the pumping tests (Data Distribution n°4).

The geometry of these fractures, assumed to be planar, is described in two slightly different documents:

- Wikberg et al. (1991, p.97) listed 16 fractures in 1991 characterised by traces at the outcrop, and their dip.
- 22 fractures [Fig. 3-1] are listed in a technical note of February 15, 1993. Each is identified by three points, two at the outcrop and one underground, corresponding to the lowest point where the fracture is intersected by the wells. When no information exists on the lateral and vertical extension of these fractures, the following assumptions are made:
 - vertical and lateral extensions reach the boundaries of the zone studied [Fig. 3-2]. The extension of the fractures, not quantified, may be assumed from the piezometric drop measured on neighbouring islands while drilling the underground laboratory gallery.
 - the fractures are assumed to have a large extension. We assume therefore that they go beyond their intersections with other fractures. Nevertheless, when this is not verified at the outcrop, we admit that the same is true at depth and that the first fracture runs up against the second, regardless of the depth.
- Little information is available concerning the distribution of salinity; we assume that under the sea (hence on the vertical boundaries of the domain), it follows the equation $S = 7 + 0.012 z$ where S is the salinity in g/l and z is the depth below sea level in m.
- Although Äspö Island is only separated from the neighbouring islands and the continent by shallow inlets of water, the conceptual model assumes a hydrostatic distribution of hydraulic heads at the lateral limits of the model: the eventual occurrence of regional flow is neglected as if these water inlets were able to

Figure 3-1

Main Identified fractured zones

(Names, dips and directions)

EW-1a (60°, NW)	NE-3a (80°, NW)
EW-1b (88°, NW)	NE-3b (70°, NW)
EW-1c (78°, SE)	NE-4a (71°, SE)
EW-1d (75°, NW)	NE-4b (78°, SE)
EW-3 (79°, S)	NW-1 (30°, NE)
EW-5 (37°, N)	NNW-1 (Vertic.)
EW-7b (81°, SE)	NNW-2 (Vertic.)
EW-7a (52°, SE)	NNW-3 (Vertic.)
NE-1a (70°, NW)	NNW-4 (Vertic.)
NE-1b (75°, NW)	NNW-5 (Vertic.)
NE-2 (78°, NW)	NNw-6 (Vertic.)

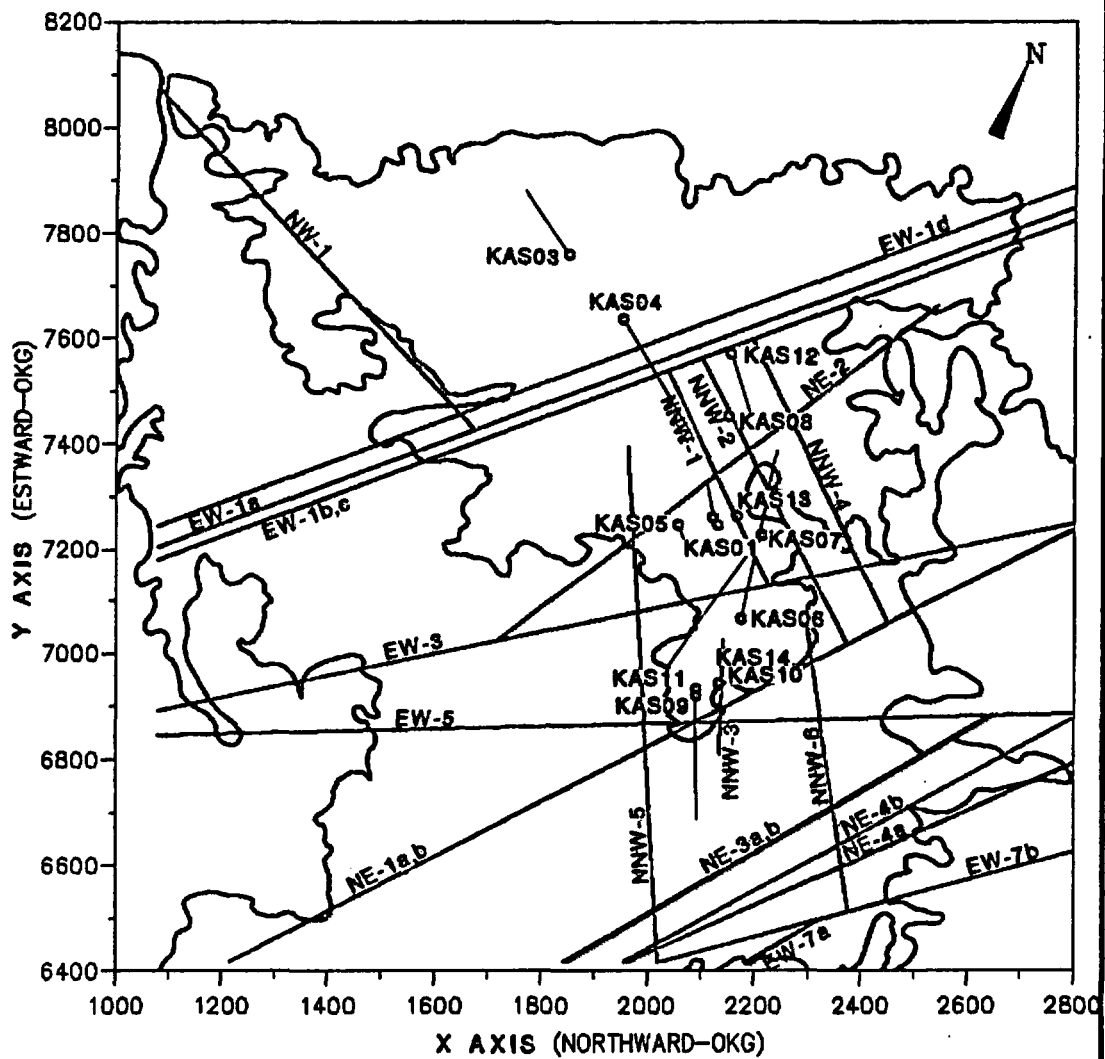
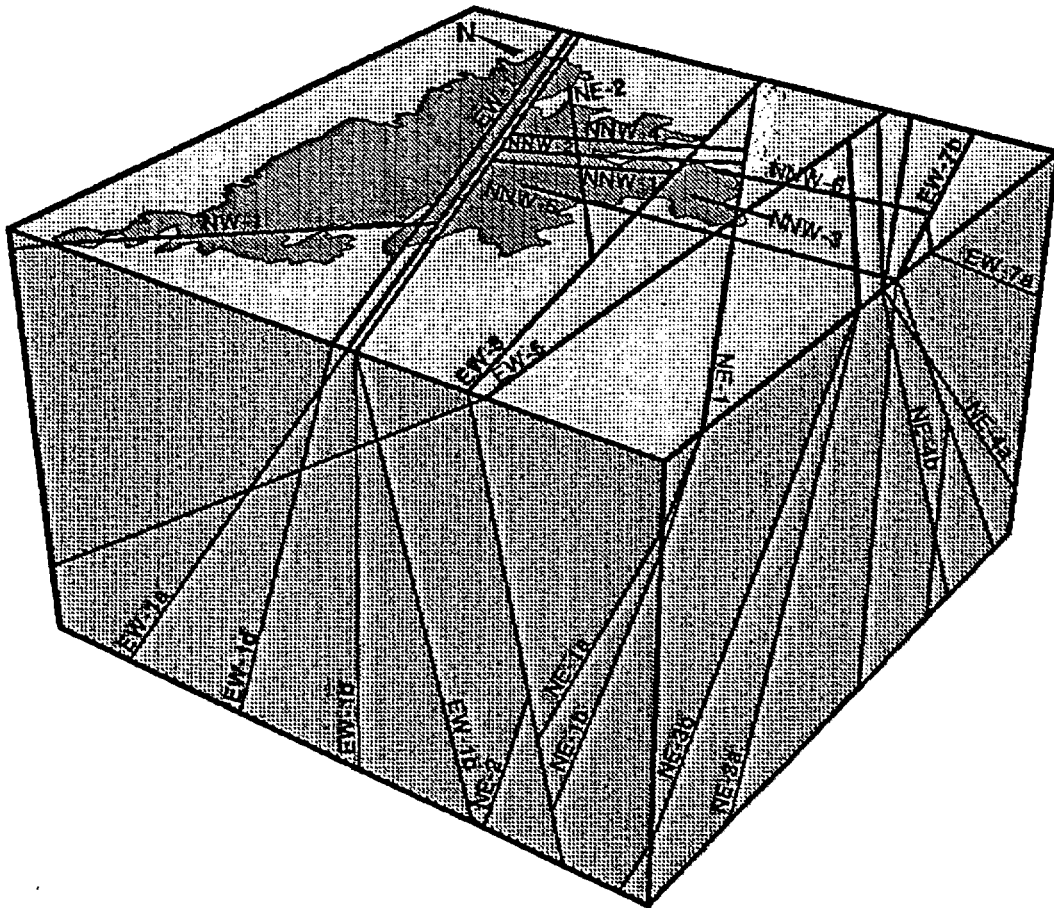


Figure 3-2

Fractured zones 3D view

(Names, dips and directions)

EW-1a (60°, NW)	NE-3a (80°, NW)
EW-1b (88°, NW)	NE-3b (70°, NW)
EW-1c (78°, SE)	NE-4a (71°, SE)
EW-1d (75°, NW)	NE-4b (78°, SE)
EW-3 (79°, S)	NW-1 (30°, NE)
EW-5 (37°, N)	NNW-1 (Vertic.)
EW-7b (81°, SE)	NNW-2 (Vertic.)
EW-7a (52°, SE)	NNW-3 (Vertic.)
NE-1a (70°, NW)	NNW-4 (Vertic.)
NE-1b (75°, NW)	NNW-5 (Vertic.)
NE-2 (78°, NW)	NNw-6 (Vertic.)



impose their head over the vertical. The impact of this approximation remains to be determined.

- Recharge by precipitation on Äspö Island, calculated by various hydroclimatic methods, is estimated at between 128 and 218 mm/yr (Svensson, 1987).
- It is considered that the groundwater flow regime was under steady state, before the pumping tests. Little data exists concerning piezometric fluctuations linked to tides or seasonal rainfall.
- There are no other pumping wells than those used for the tests.

4. DEVELOPMENT OF THE NUMERICAL MODEL OF ÄSPÖ

In order to be coherent with previous works performed by SKB, we chose to start, using MARTHE, with the same conceptual model as described above. Only few modifications have been introduced afterwards.

4.1 AREAL EXTENT OF THE ZONE MODELLED

The area modelled [Fig. 4-1] includes all of Äspö Island with boundaries parallel to the OKG coordinate system. The parallelepiped thus outlined has horizontal dimensions of 1800 m x 1800 m and a vertical extension of 1235 m.

4.2 THE GRID

The structure is a regular 3-D grid made up of parallelepipeds organized in 24 horizontal layers; their projection in the horizontal plane consists in 29 lines and 28 rows of rectangular elements [Fig. 4-1]. The thickness of the layers increases progressively from 10 m at surface level, up to 80 m below -500 m. At depths of between 35 and 515 m, 12 layers 40 m thick represent the zone intersected by the shaft and the pumping tests. Horizontally the finer mesh (40 m x 40 m) is defined in the southeastern part of the island where the pumping wells of LPT1 and LPT2 are located; it augments progressively, up to 160 m x 160 m.

In all, there are 19,488 parallelepipedic cells. A choice of smaller cells such as 20 m cubes would have led to a grid of nearly 100,000 cells.

4.3 DISTRIBUTION OF EXCHANGE COEFFICIENTS BETWEEN CELLS

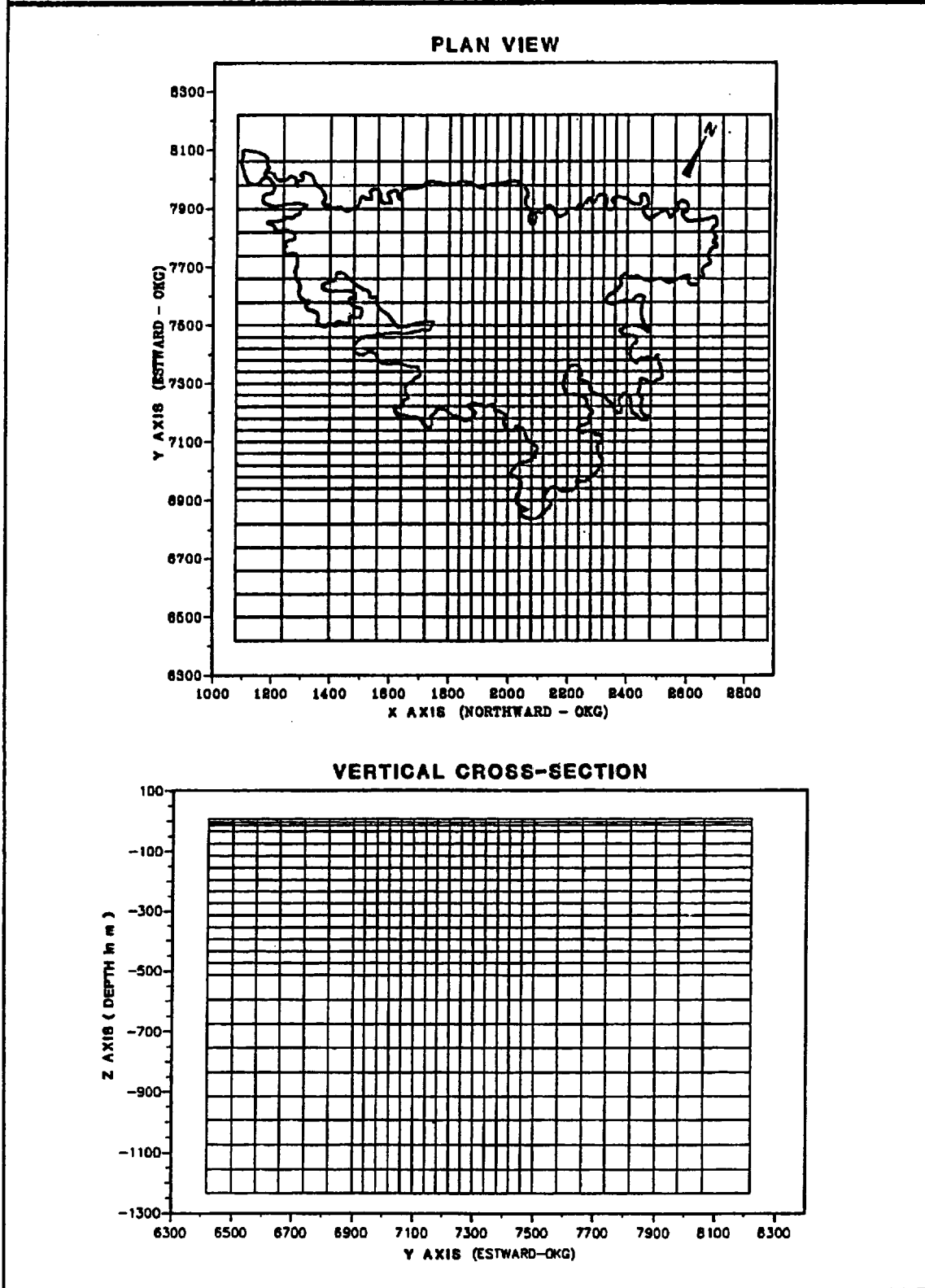
As mentioned in paragraph 3.3, groundwater flow in the fractures was accounted for using exchange coefficients between cells. These were calculated by the superimposing of fracture transmissivities on a homogeneous matrix permeability of 10^{-8} m/s. 22 fractures (Data Distribution n°4) were positioned corresponding to 1993 data, with their initial transmissivities resulting from SKB interpretations.

4.4 BOUNDARY CONDITIONS

The boundary conditions, which were not modified during the simulations, are of 2 types: either fixed head or fixed flow (including pumping wells inside the domain). When water enters the model (positive inflow of the rain infiltration) or is susceptible to enter (fixed head boundary), it is necessary to indicate the concentration (or salinity) of this water.

Figure 4-1

Simulation grid



4.4.1 Lower boundary

The lower boundary is a no flow boundary. In the first runs it was a fixed density limit, but the change to a real no flow boundary with computed density did not modify significantly the results.

4.4.2 Lateral boundaries and upper boundary (except for the Island).

The head is fixed [Fig. 4-2] on the lateral boundaries (hydrostatic head in equilibrium with sea water), and the part of the upper boundary which is the Baltic sea bottom (-20 m). As water is susceptible to enter the model through these surfaces according to the locally computed head gradient, the model must have information on the salinity $S(\text{g/l})$, and a law to deduce density. Adopting SKB assumptions,

- salinity (g/l) is given as a function of depth $z(\text{m})$ under sea level, according to the equation $S = 7 + 0.012 z$.
- and the density of sea water is approximately related to the salinity $S(\text{g/l})$ by the equation $d = 1 + 6.84 \cdot 10^{-4} S$.

4.4.3 Upper boundary (Island of Äspö).

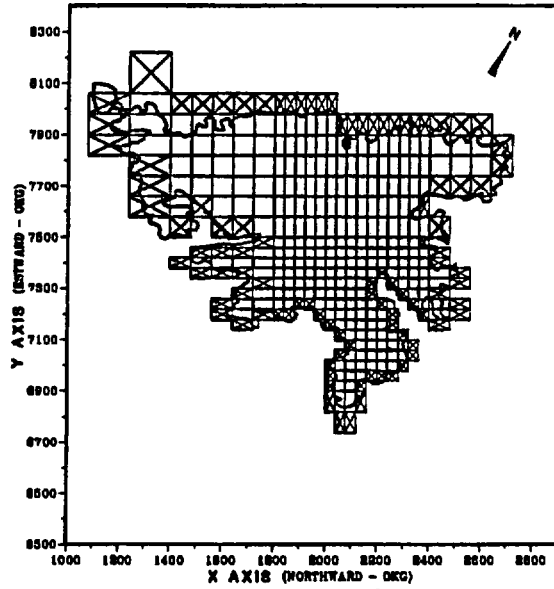
The surface of the Island of Äspö itself is a fixed flux boundary, corresponding to the infiltration of the rain into the granitic body. This rain inflow has a density of 1.

Figure 4-2

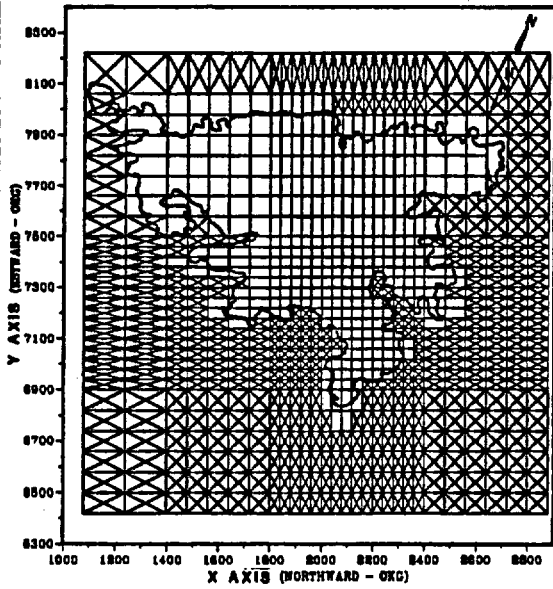
Simulated domain and hydraulic boundary conditions

- ☒ Grid block with fixed head
- ☐ Grid block

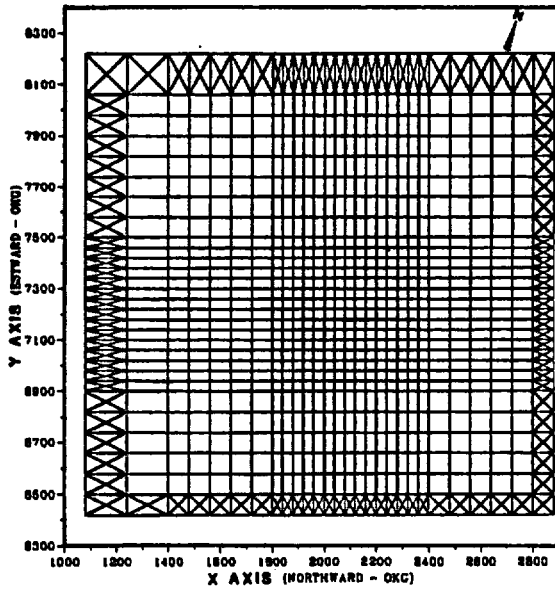
LAYER 1 (Plan view)



LAYER 2 (Plan view)



LAYERS 3 TO 24 (Plan view)



5. MODELLING STEADY STATE CONDITIONS

For this we must determine how much the conceptual model of Äspö Island described in paragraph 2 is coherent with both the piezometric map under natural flow and the salinity measured in wells.

5.1 NUMERICAL METHODS ADOPTED

For simulations of the Äspö Island site, the following options were adopted:

- Flow was computed with piezometric head rather than pressure in order to ensure a better precision.
- For the same reason, density is expressed as relative density in relation to water and in thousandths. For example, a density of 1.007 is stored in the form 7 for the calculation of mass fluxes.
- The system of equations for flow is solved with the conjugate gradient method with incomplete Cholesky preconditioning.
- Mass transfer is computed as a purely convective process, using Gauss-Seidel iteration.

An excellent convergence of calculations can be reached, provided we take the precaution to use a very low under-relaxation factor during density calculations (≈ 0.001). The flow balance reaches equilibrium at $\pm 0.03\%$, while the mass balance of salinities reaches equilibrium at $\pm 1\%$.

5.2 SIMULATIONS

The large differences in permeability measured between the matrix and the fractures made the convergence of calculations difficult when we superimposed the 22 fractures identified in Äspö Island on the matrix all at once. In order to solve this problem, we introduced the fractures into the grid progressively. This also allowed us to study the hydraulic role played by the different fractures.

We introduced first 2, then 3, 7, 14, and finally 22 fractures into the grid.

The basic simulation conditions were the following:

- a homogeneous matrix with uniform permeability of 10^{-8} m/s intersected by an increasing number of fractures.
- recharge from precipitation: 3 mm/yr

- the equation $S = 7 + 0.012 z$ controlling the evolution of salinity with depth on lateral boundaries.
- SKB's values for the transmissivity of fractures.

While not questioning the high transmissivity of $2 \cdot 10^{-5} \text{ m}^2/\text{s}$ estimated for fracture EW-1, one sees that due to the relatively small extent of the model (with supposedly uninfluenced heads on its lateral boundaries), it introduces a strong connection between the inner part of the model and these boundaries. In general, the fractures reaching these limits play an excessive draining role, with unlimited supply of water. In order to compensate this artefact, and following Svensson approach, the permeability of the fractures have been lowered close to the lateral boundaries, which is equivalent to move the limits further away.

Figures 5-1 and 5-2 give results of the stage where 7 fractures were introduced and the final stage where 22 fractures were introduced. A comparison between these two figures shows the drainage effect of the fractures. Adding new conductive fractures decreases hydraulic heads and ascent the freshwater/salt water interface. In the final configuration, with 22 fractures, one observes an under-estimation of head of around one meter for the piezometric dome in the northwest of the island. Several solutions are possible to correct these deviations, some having a global effect (increase recharge rate, decrease matrix permeability, etc.), others a local effect (decrease transmissivities of the fractures, extend the fractures farther, etc.). In this first stage of modelling, we increased the recharge rate. Other parameters will be varied during calibration under transient conditions of pumping tests LPT1 and LPT2. With an infiltration rate of 5.5 mm/yr, the piezometric dome in the northwest of the island is rather well described [figure 5-3], while in the south of the island where the observed piezometry is somewhat disrupted, the calculated levels are nevertheless coherent with measured values.

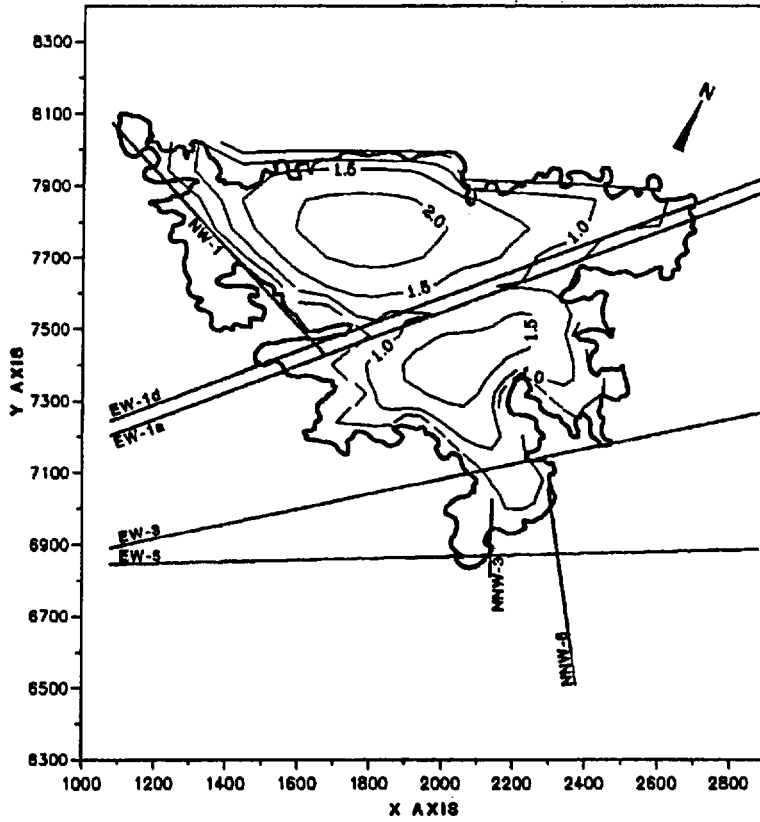
Concerning salinity, the comparison of values calculated with MARTHE with those measured in the field is generally satisfactory, in spite of some local differences [Table 5-1]. These can be of diverse origin:

- A rather coarse spatial discretisation which would explain deviations in salinity of several g/l near the freshwater/salt water interface, depending on the position of the observation point relatively to the cell.
- Vertical flow along fractured zones, which might locally alter the salinity distribution. This has been revealed by in situ measurements. It would be unrealistic to attempt to model the complexity of such a phenomenon by a regional model.

Figure 5-1

Scenario with 7 fractures and 3mm/year infiltration rate

Contour lines for head at surface



Contour lines for concentration (g/l) at cross-section X=2140 OKG

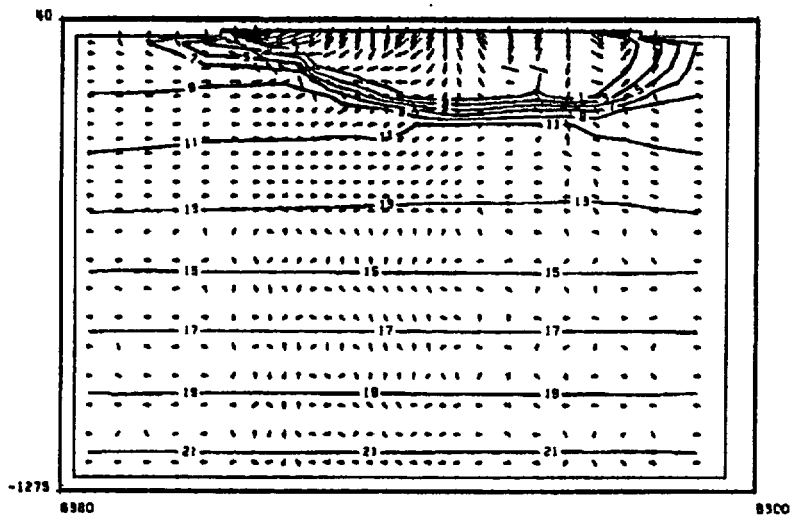
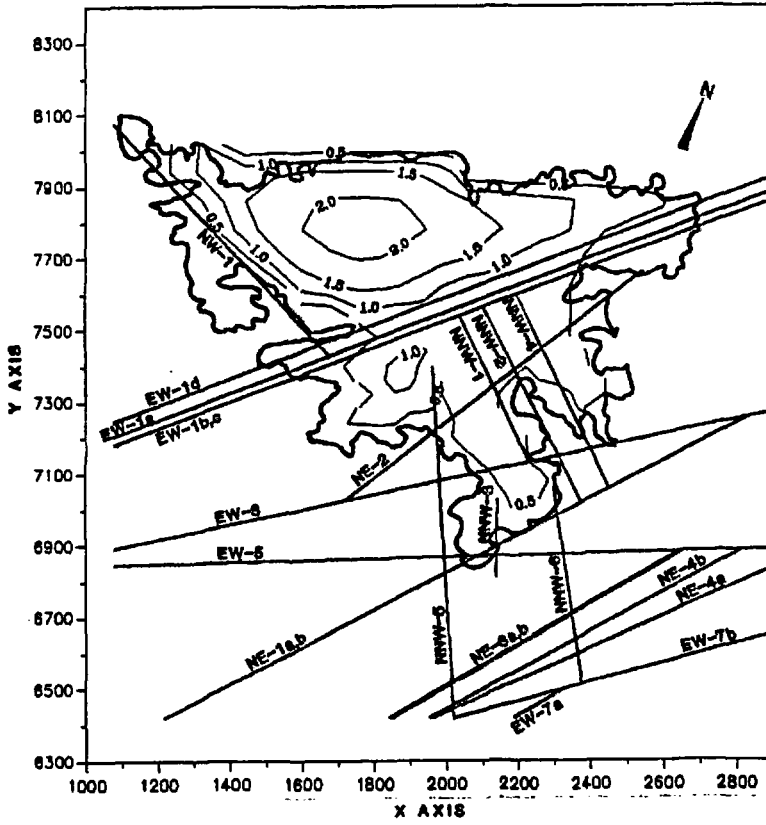


Figure 5-2

Scenario with 22 fractures and 3mm/year infiltration rate

Contour lines for head at surface



Contour lines for concentration (g/l) at cross-section X = 2140 OKG

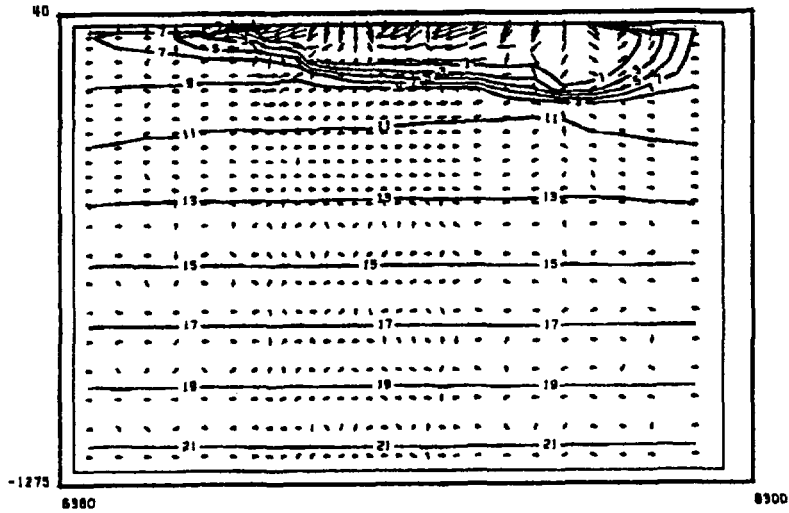
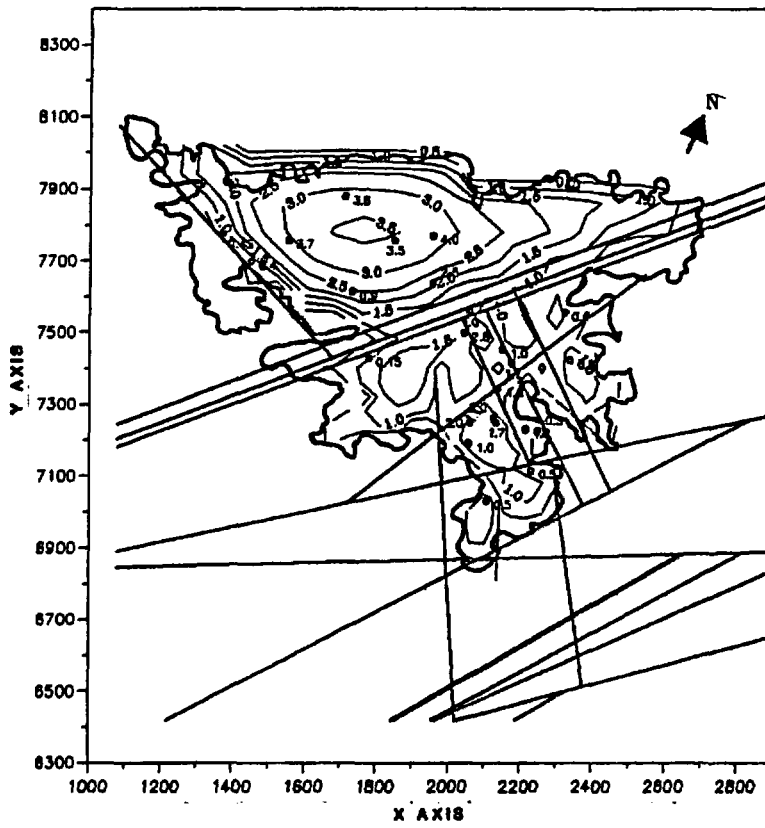


Figure 5-3

Scenario with 22 fractures and 5.6mm/year infiltration rate

Contour lines for head at surface



Contour lines for concentration (g/l) at cross-section X=2140 OKG

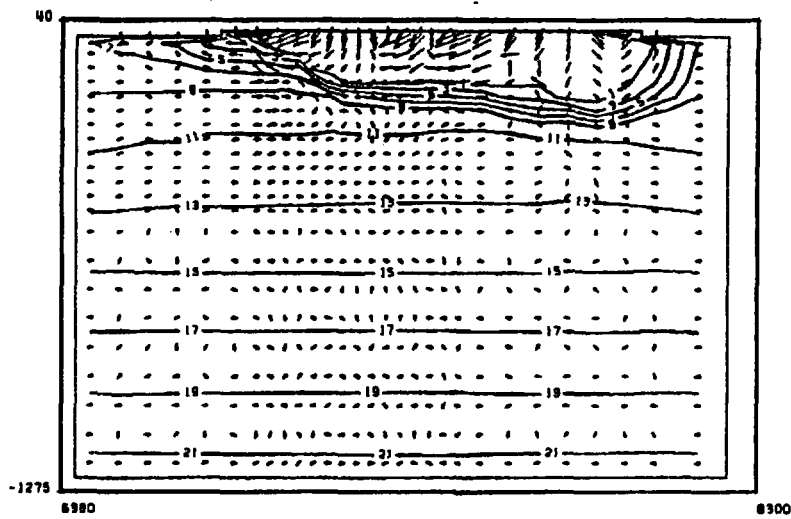


Table 5-1		Measured and simulated salinities	
Observation section	Depth (m)	Field measurement S(g/l)	MARTHE simulation S(g/l)
K02-B6	52.00	4.400	0.
K02-B5	189.00	7.200	6.41
K02-B4	309.00	9.500	11.18
K02-B3	537.00	9.800	13.82
K02-B2	824.00	14.200	16.50
K02-B1	873.00	15.800	17.60
K03-C6	51.00	2.100	0.
K03-C5	210.00	2.200	0.
K03-C4	346.00	8.600	10.70
K03-C3	514.00	9.000	13.15
K03-C2	604.00	6.600	14.59
K04-D6	139.00	0.500	0.18
K04-D5	149.00	1.000	0.18
K04-D4	188.00	1.200	2.32
K04-D3	235.00	2.500	7.15
K04-D2	276.00	5.300	10.71
K04-D1	340.00	9.300	11.49
K05-E5	81.00	0.800	0.
K05-E4	263.00	1.200	10.30
K05-E3	312.00	6.200	11.18
K05-E2	426.00	7.800	12.31
K05-E1	456.00	8.900	12.79
K06-F6	81.00	3.200	0.
K06-F5	180.00	4.900	7.52
K06-F4	260.00	10.300	10.70
K06-F3	295.00	10.000	11.14
K06-F2	333.00	10.800	11.46
K06-F1	374.00	10.800	11.98
K07-J6	47.00	2.900	0.
K07-J5	104.00	5.200	0.
K07-J4	206.00	6.300	10.18
K07-J3	295.00	8.900	11.19
K07-J2	363.00	10.500	11.90
K07-J1	470.00	10.500	12.75
K08-M4	52.00	7.000	0.
K08-M3	147.00	6.600	2.20
K08-M2	314.00	9.000	11.15
K08-M1	455.00	10.200	12.79

5.3

CONCLUSIONS OF THE STEADY STATE STAGE

The tool developed to model the low permeability and fractured granitic environment on Äspö Island gives results in agreement for both the piezometry calculated at the surface and the salinity calculated underground. The estimated recharge from precipitation (5.5 mm/yr), while in agreement with Svensson's results (3 mm/yr), is still very low compared with results from a classic hydroclimatological analysis (between 130 and 220 mm/yr). This is very likely explained by heavy hypodermic flow which diverts rain water infiltrations from the granitic body, by superficial drainage towards the sea.

6. MODELLING TRANSIENT CONDITIONS . SIMULATION OF PUMPING TEST LPT2

This second phase provides verification of the representativity of the parameters derived from the natural, undisturbed flow regime model. It analyses the hydraulic responses to the solicitations imposed by the long term pumping test LPT2 and by comparing them to the numerous measurements taken in the field during the test.

6.1 LPT2 PUMPING TEST

A pumping test was carried out in well KAS06, over the whole length of the well (no packer in this well). The monitoring network included 33 wells, scattered all over the island [Fig. 6-1]; in these wells around 100 measurement sections were isolated between packers. Lasting 92 days, the test was done with 3 successive steps with a constant discharge rate [Fig. 6-1]. Head was measured on all of the sections. Figure 6-1 gives, as an example, the evolution of the drawdown at the pumping well. The pumping influenced almost all of the island except for the extreme northwestern corner, isolated by the four fractures EW-1a to EW-1d.

6.2 ASSUMPTIONS FOR MODEL CALCULATIONS

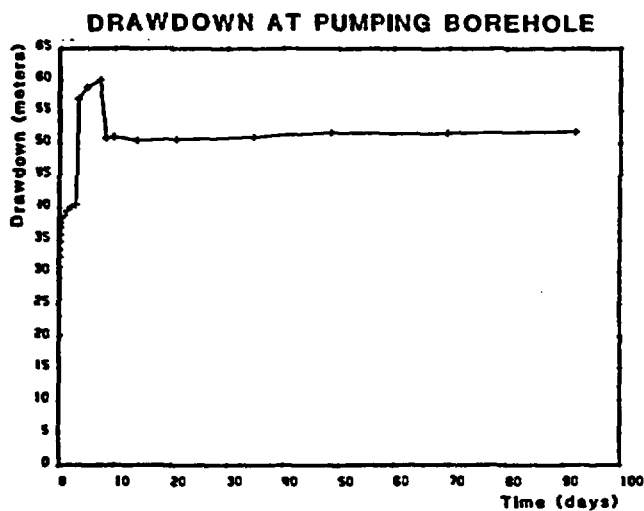
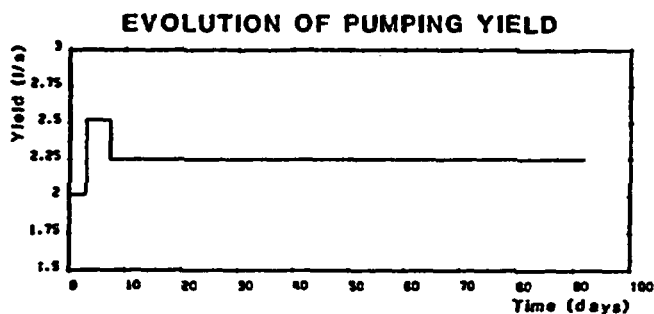
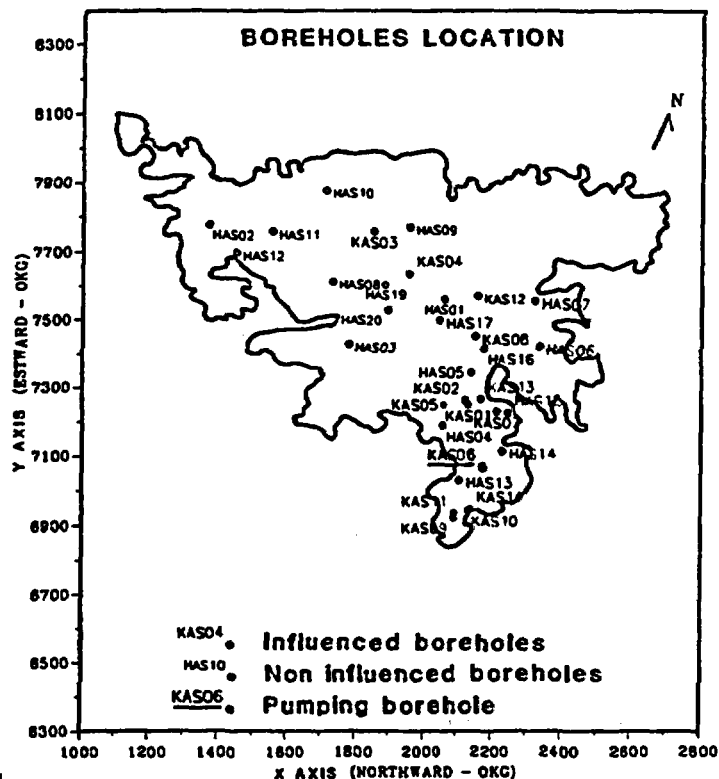
The first simulation is performed keeping unmodified the parameters obtained from the simulations under natural flow regime (matrix permeability, transmissivity of fractures, infiltration, boundary conditions). Pumping is simulated by distributing the pumping rate, measured during spinner test, amongst the four cells located at the intersections of the well and the four conductive faults which intersect it [Table 6-1]. As fracture EW-X is not described in the conceptual model, and consequently not modelled with MARTHE, its contribution to the total pumped discharge rate is distributed between the other fractured zones identified in the conceptual model.

Table 6-1. Distribution of inflow in well KAS06

Fracture	Measured discharge (%)	MARTHE simulated discharge (%)
EW-3	15	16
NNW-1	20.9	22
EW-5	33.5	34
NNW-2	25.8	28
EW-X	4.8	—

Figure 6-1

LPT2 Pumping test



RESULTS

The first simulation of the LPT2 pumping test, followed by an analysis of the sensitivity of the calibration parameters around this initial solution, revealed the following:

- Confirmation of the need to extend the boundary of the model by imposing lower fracture transmissivity values ($10^{-7} \text{ m}^2/\text{s}$) where they intersect the lateral boundaries of the model.
- Need, though less marked, to decrease the vertical permeability of the fractures at their intersection with the floor of the Baltic Sea (upper limit of the model) by imposing a vertical anisotropy K_V/K_H of 0.1 on the second layer of the model, in order to simulate a possible clogging of the fractures by marine sediments.
- Confirmation of the assumption that on the time scale of the pumping test, the density field varies very little with time.
- Need for occasional readjustment of the transmissivity of two fractures:
 - EW-3, with $10^{-5} \text{ m}^2/\text{s}$ (instead of $5 \cdot 10^{-7}$),
 - NE-1a and NE-1b with $10^{-5} \text{ m}^2/\text{s}$ (instead of 10^{-4}).
- The value of 4% was kept for the free storage coefficient (especially first layer); sensitivity studies have shown that this parameter is not very influent (results obtained with free storage of 2 and 5% are not basically different).
- Attribution of a specific storage coefficient S_s of $5 \cdot 10^{-8} \text{ m}^{-1}$ for the other layers (captive aquifer); other values between 10^{-8} m^{-1} and $5 \cdot 10^{-7} \text{ m}^{-1}$ give also consistent results.

Table 6-2 gives fracture transmissivity values calibrated from these simulations.

Table 6-2 Transmissivities of the main fractured zones

Fracture zone	Dip	Transmissivity ($10^{-5} \text{ m}^2/\text{s}$)		
		SKB average	SKB interval	MARTHE calibration
EW-1a	60°NW	2.00	-	2.00
EW-1b	88°NW			0.05
EW-1c	78°SE			0.05
EW-1d	75°NW			0.05
NE-2	78°NE	0.40	0.2-1.0	0.40
EW-3	79°S	0.05	0.01-0.1	1.00
EW-5	37°N	2.00	1.0-4.0	2.00
NE-1a	70°NW	20.00	4.0-40.0	1.00
NE-1b	75°NW	20.00	4.0-40.0	1.00
NE-3	70°NW	3.00	-	1.50
NE-3	80°NW			1.50
NE-4	78°SE	35.00	-	16.00
NE-4	71°SE			16.00
NNW-1	verticale	1.50	0.5-2.0	1.50
NNW-2	verticale	4.00	2.0-6.0	4.00
NNW-3	verticale	2.00	0.5-5.0	2.00
NNW-4	verticale	4.00	2.0-6.0	4.00
NNW-5	verticale	5.00	1.0-10.0	5.00
NNW-6	verticale	5.00	1.0-10.0	5.00
NW-1	30°NE	0.70	-	0.70
EW-7a	81°SE	14.00	-	7.00
EW-7b	54°SE			7.00

Modelling of the LPT2 pumping test with the above hypotheses brings the following comments:

- Rather good general agreement between measured and simulated drawdowns, in particular for sections intersecting fractures EW-3, EW-5 and NNW-2 which are pumped directly and for fracture NE-2.
- Locally, substantial under-estimation, as was also observed by Svensson, of some simulated drawdowns, notably in the sections intersected by fracture NNW-1.
- Clear differentiation and agreement of wells influenced by pumping and those which are not influenced.

Figures 6-2 and 6-3 give the results obtained for four typical measurement sections. Figure 6-4 shows comparisons of measured and simulated drawdown for all of the sections at the end of the pumping test.

6.4 VERIFICATION AGAINST THE DATA OF THE PUMPING TEST LPT1

An earlier pumping test, lasting 50 days, was done in well KAS07 over the whole length of the well. The discharge rate was maintained constant at 1.25 l/s. The monitoring network included 68 measurement sections in 24 wells. Two specific problems make interpretation of the results difficult: the distribution of inflow along the length of the pumping well was not measured as during LPT2 test, and there is a large imprecision on head values measured between packers (from ± 0.15 m to ± 1.30 m according to Ekman). These are the reasons why the study has been mainly dedicated to the interpretation of LPT2.

One run has been carried out, using the same numerical model as for LPT2, and distributing the pumped flow proportionally to the transmissivity of the fractures intersected; it shows that all of the drawdowns are under-estimated. The contrast between influenced and non influenced wells is nevertheless correctly reproduced.

6.5 CONCLUSIONS ON FLOW MODELLING.

Aside from some occasional readjustments of fracture transmissivities, the parameters and characteristics of the model after the transient stage are identical to those obtained from modelling under natural flow regime. The results are globally satisfactory in spite of the fact that locally there are still some significant differences in the order of magnitude of a little number of drawdowns.

Nevertheless, the uniqueness of the model is uncertain, since the effective recharge from precipitation is much lower than the total infiltration calculated with hydroclimatological analysis, probably because an important portion of the flow escapes through the zone of superficial weathered granit. The reduction of permeabilities of the fractures, close to lateral and upper boundaries, is necessary, but cannot be strictly defined. Uncertainty also lies on the matrix permeability: different values can be adopted, provided the infiltration rate on the one hand and the distribution of transmissivities in fractures on the other hand are adapted.

However, globally, it appears that the SKB conceptual model is a good compromise, and modelling it with MARTHE yields reasonable fit to the measures, with parameters close to those of SKB's model. One way to improve this model should be to introduce one or several sub-vertical fractures EW-X intersecting the bottom of KAS06. Such fractures should cross NNW-1, NNW-2 and NNW-4, increasing hydraulic connections in this area and allowing greater simulated drawdowns for LPT1 pumping test.

Figure 6-2

Observed/simulated drawdowns
Sections KAS02-B4 and KAS04-D1

Observed drawdowns

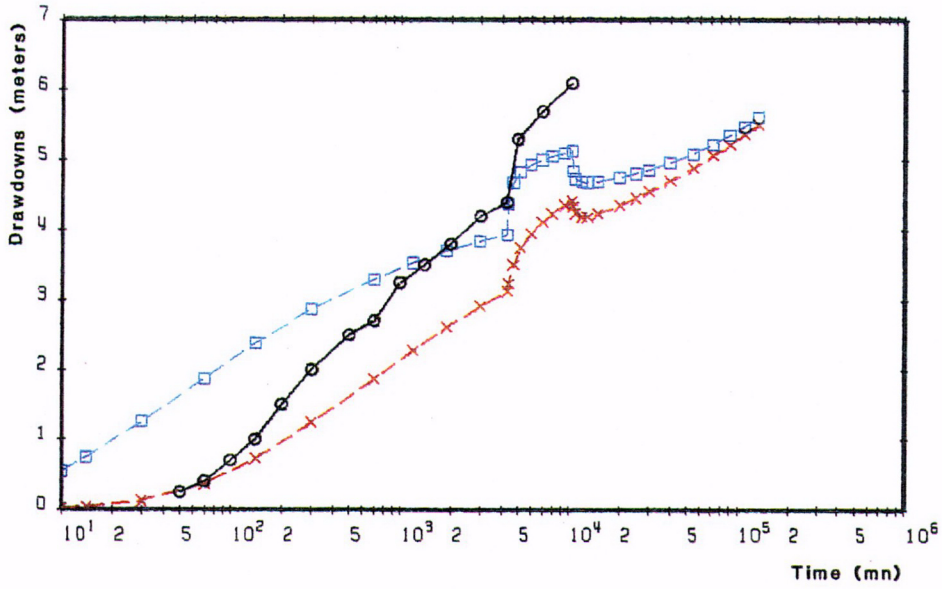
Simulated drawdowns

--- $S_s = 2 \cdot 10^{-7}$ (m-1)

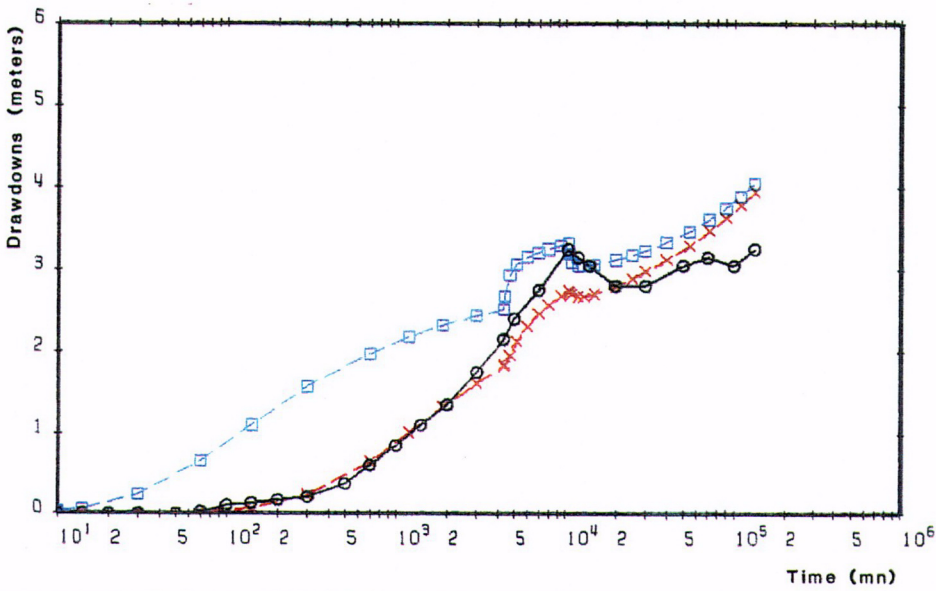
--- $S_s = 5 \cdot 10^{-8}$ (m-1)

Z : Measured section elevation

Section KAS02-B4 (Fracture 6 : EW5) Z = -309



Section KAS04-D1 (Fracture 11 : NE2) Z = -340



C-01

Figure 6-3

Observed/simulated drawdowns
Sections KAS07-J4 and KAS08-M3

Observed drawdowns

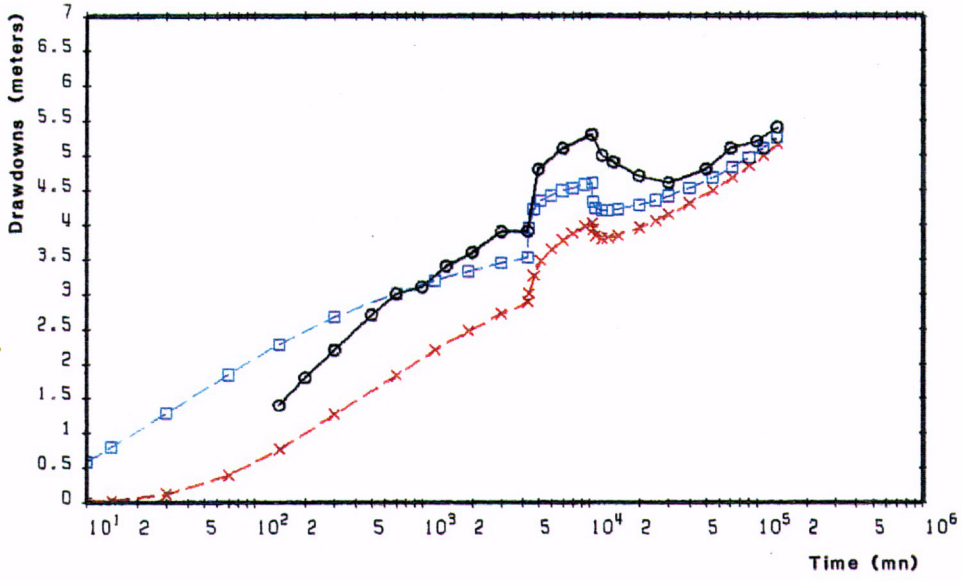
Simulated drawdowns

--- $S_s = 2.10^{-7} \text{ (m}^{-1}\text{)}$

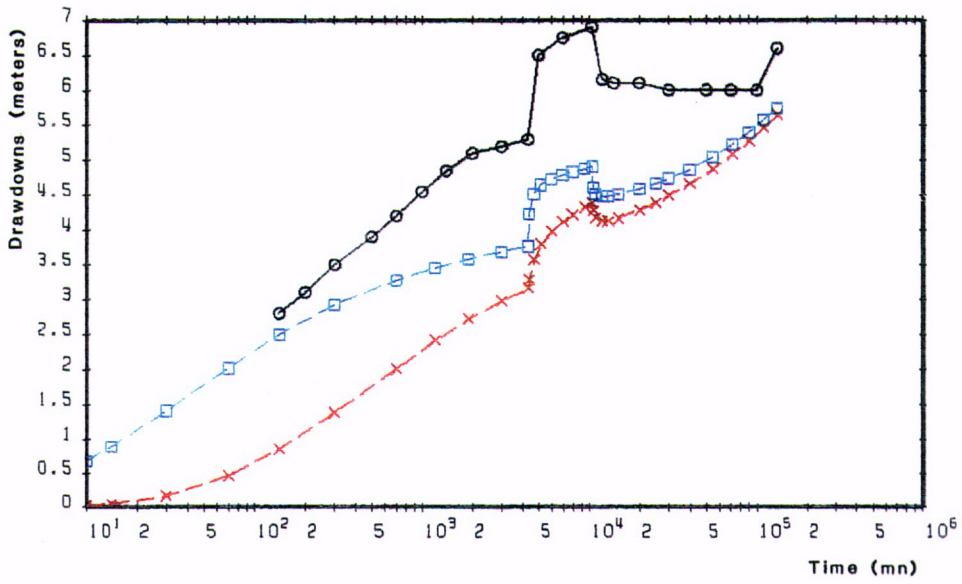
- - - $S_s = 5.10^{-8} \text{ (m}^{-1}\text{)}$

Z : Measured section elevation

Section KAS07-J4 (Fracture 6 : EW5) Z = -205



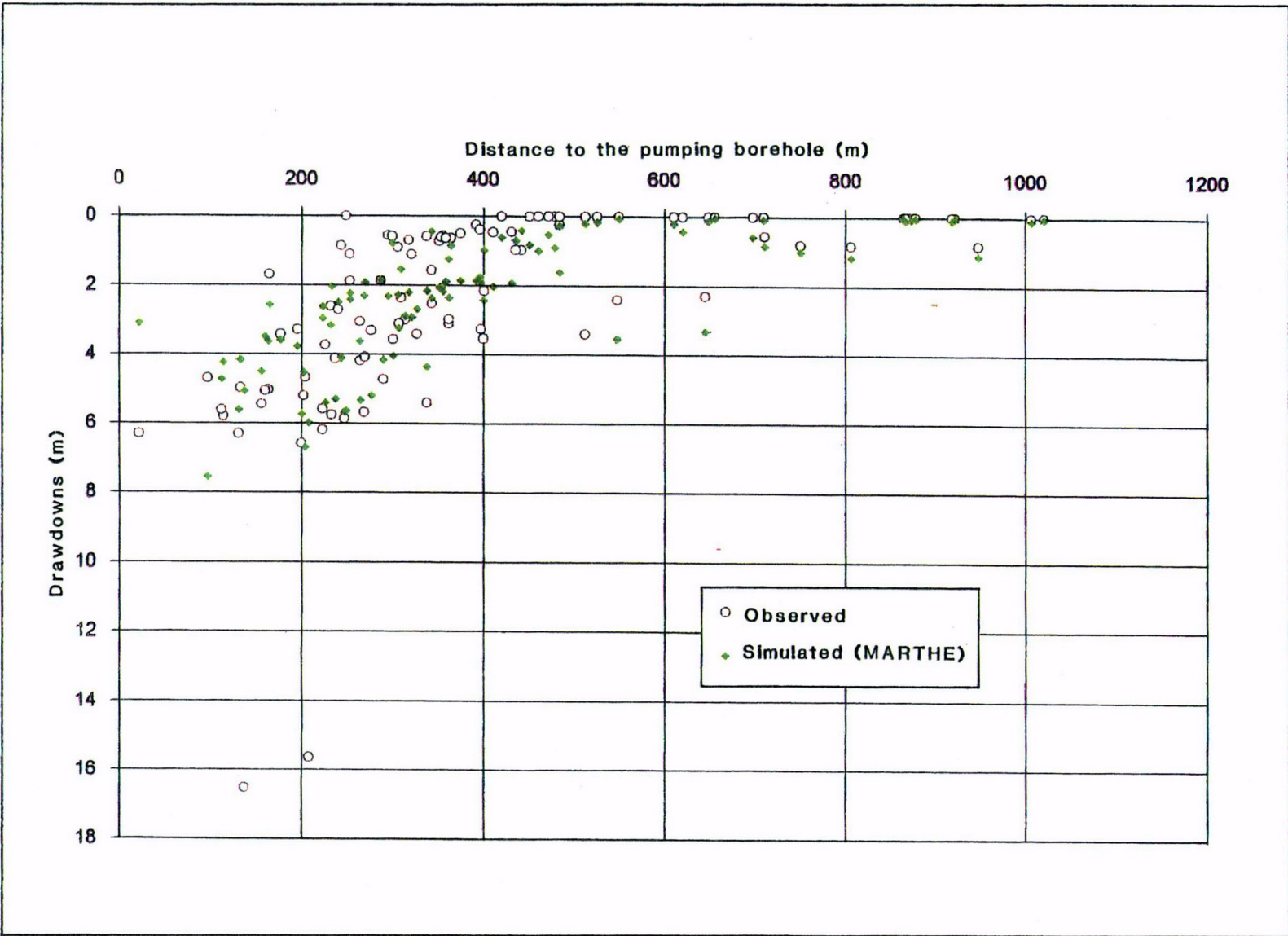
Section KAS08-M3 (Fracture 18 : NNW2) Z = -147



C-02

Figure 6-4

Comparison between observed and simulated drawdowns at the end of LPT2 test



C-03

7. MODELLING OF TRACER EXPERIMENTS

7.1 EXPERIMENTAL CONDITIONS

Six tracer experiments were done between day 16 and day 92 of the pumping test LPT2, with a constant discharge rate of 2.25 l/s and practically steady piezometric levels. The tracers were injected by pulses separated by intervals of 3 or 6 days in injection sections chosen to coincide with all of the fractures intersected by the well KAS06: NNW-1, NNW-2 and EW-5. The location of the injection boreholes is presented in Figure 7-1. Table 7-1 shows the characteristics of the tracer experiments carried out (time origin is chosen at the beginning of the first tracer injection, 396 hours after the beginning of the LPT2 pumping test).

Table 7-1 Tracer Experiments. Main characteristics

Tracer	Section	Time of injection (h)	Injection flow rate (ml/mn)	Volume injected (l)	Number of pulses	Interval between pulses (d)	Fracture intersected
Uranine	KAS12-DB	0	12.0	5	7	3	NE-2 or EW-5
Rhenium	KAS08-M1	0	9.5	4	7	3	NE-1
Indium	KAS02-B4	4	12.5	4	1	--	EW-5
Iodine	KAS07-J4	6	4.9	4	4	6	EW-5
Rhenium	KAS08-M3	677	9.7	4	1	--	NNW-2
Uranine	KAS05-E3	678	27.9	25	1	--	EW-5

Of the four tracers injected, only Uranine and Rhenium (respectively injected in wells KAS12 + KAS05 and KAS08) reached the pumping well, with a recovery rate of 28% and 30%, respectively.

The quantities injected (the units are g for Uranine and Bq for Rhenium) at each pulse are given in Table 7-2.

Table 7-2 Quantity releases

Tracer	Injection section	Injection pulse	Beginning of injection (h)	Quantities released (g or Bq)	
Uranine	KAS12-DB	1	0	30.7	total = 303.8 g
		2	73	28.4	
		3	144	79.6	
		4	222	75.2	
		5	288	30.6	
		6	366	28.1	
		7	432	31.2	
Uranine	KAS05-E3	1	678	238	
Rhenium	KAS08-M1	1	0	$1.76 \cdot 10^9$	total = $1.12 \cdot 10^{10}$ Bq
		2	72	$1.65 \cdot 10^9$	
		3	140	$3.66 \cdot 10^8$	
		4	216	$1.17 \cdot 10^9$	
		5	284	$1.83 \cdot 10^9$	
		6	359	$2.17 \cdot 10^9$	
		7	431	$2.27 \cdot 10^9$	
Rhenium	KAS08-M3	1	677	$8.40 \cdot 10^9$	

Concentrations are measured from samples taken at different levels of the producing well KAS06, but concentration in the well at the level of its intersection with a given fracture is a mixture of the fracture inflow, with all the inflows collected at lower levels. In order to determine the breakthrough curve (BTC) of each inflow, it is then necessary to discriminate the contribution of other fractures. The knowledge of the inflow coming from each fracture is necessary for that purpose; it has been measured by a spinner test. It is clear that, as these BTCs result from a differentiation method, they cannot be very precise. In consequence, the hydrodispersive parameters identified from these curves, can be affected by significant imprecision; their representativity is also weakened by the fact that the recovery of the injected tracer is only of the order of 28%-30% for 2 tracers, and 0% for the others.

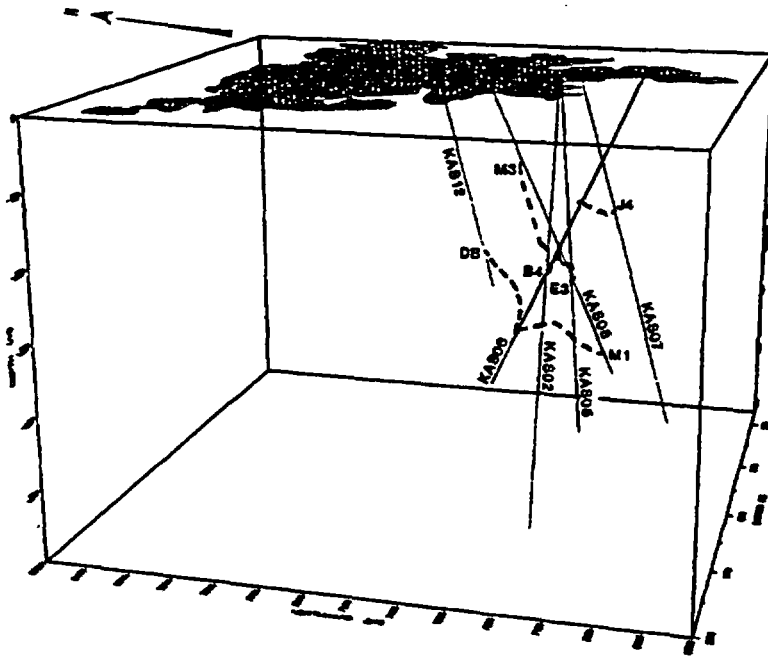
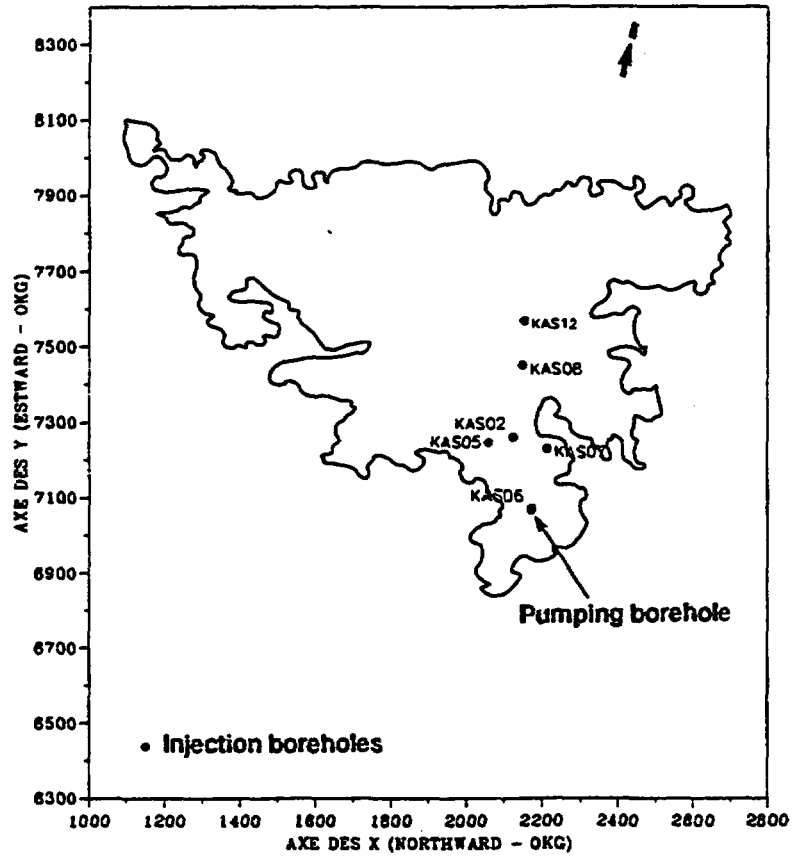
7.2 MODELLING OF THE TRACER TESTS

7.2.1 Numerical options selected for this simulation

A continuum transport model has been built, using the code SESAME with the fluxes evaluated by MARTHE. Due to the high contrast of permeabilities, and thus of groundwater velocities, between matrix and fractures, actually comes out a single porosity model representing mainly the fracture flow with an average kinematic porosity.

Figure 7-1

Tracer tests. Location of injection boreholes.
Simulated flow paths



----- Simulated flow paths

7.2.2 Modelling of flow paths

The six flow paths computed by SESAME, from injection sections to pumping borehole KAS06, are presented in Figure 7-1. The angles that can be noticed on the flow paths lines are due to fractures intersections.

7.2.3 Modelling of Rhenium

We studied the series of 7 pulses injected in KAS08-M1, and one additional pulse in KAS08-M3.

Of the 8 levels of sampling in KAS06, the most reliable data are those which concern the lowest level (level 3, conductor E, NNW-2 fracture), but data are also available for levels 4 (conductor D, EW-5 fracture), 6 (conductor Ca, EW-5 fracture) and 8 (conductor A, NNW-1 fracture).

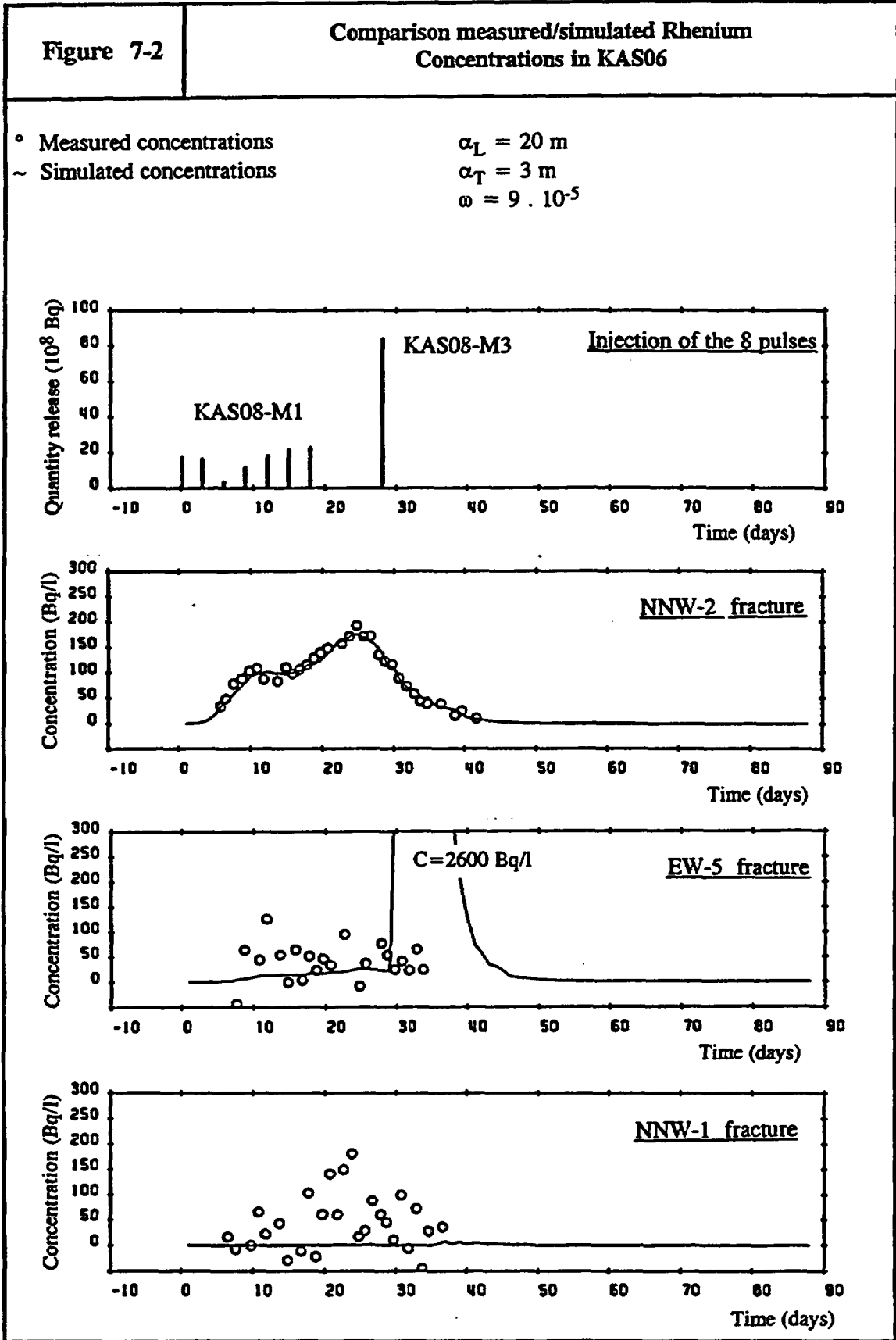
The analysis of inflow into the pumped well shows that four of the intersected conductors (B, Ca, Cb and D) belong, in fact, to the same fracture EW-5. For each of these conductors, we have the corresponding flow rate expressed as a percentage of the total pumped flow (5.6, 8.4, 4.2 and 15.3 %, respectively). We are therefore able to calculate the global BTC in EW-5 by weighted average of the various BTCs for each conductor, in proportion to the corresponding inflow. Finally, we get 3 BTCs corresponding to the levels intersected by fracture NNW-1 (conductor A), EW-5 (conductors B to D) and NNW-2 (conductor E), on which are calibrated the hydrodispersive parameters.

The time step chosen for the simulation is one day. Ten thousands particles are injected instantaneously at each pulse. The measured recovery rate (30%) is applied to the successive masses (actually to the activities) injected at each pulse.

The best fit on simulated/measured concentrations is obtained [Fig. 7-2] with the following hydrodispersive parameters: kinematic porosity = $9 \cdot 10^{-5}$, longitudinal dispersivity = 20 m and transversal dispersivity = 3 m. By taking into account the half-life of Rhenium (3.78 days), we can satisfactorily simulate the BTC measured in the pumping well for NNW-2 fracture. For EW-5 the results are not so good, but possibly the Rhenium breakthrough should have arrived later, after the end of the concentration measurements. On the other hand, for the intersection KAS06/NNW-1, the concentrations are under-estimated by a factor of at least 10 to 100, which means that one hydraulic connection between the pumping well KAS06 and the injection borehole KAS08 is not properly modelled.

7.2.4 Modelling of Uranine

The hypotheses for the model are identical to those used for Rhenium. The measured recovery rate (28%) is applied to the successive masses injected at each pulse [Table 7-2].



The results [Fig. 7-3] are satisfactory for the fractures EW-5 and NNW-2. Again, for the intersection KAS06/NNW-1, the concentrations are greatly underestimated, which means that a hydraulic connection between the pumping well KAS06 and the injection boreholes KAS12 and KAS05 is not, or insufficiently, modelled. The hydrodispersive parameters obtained are 20 m and 3 m for longitudinal and transversal dispersivities, as for Rhenium for α_L and very close for α_T , and $3 \cdot 10^{-4}$ for kinematic porosity.

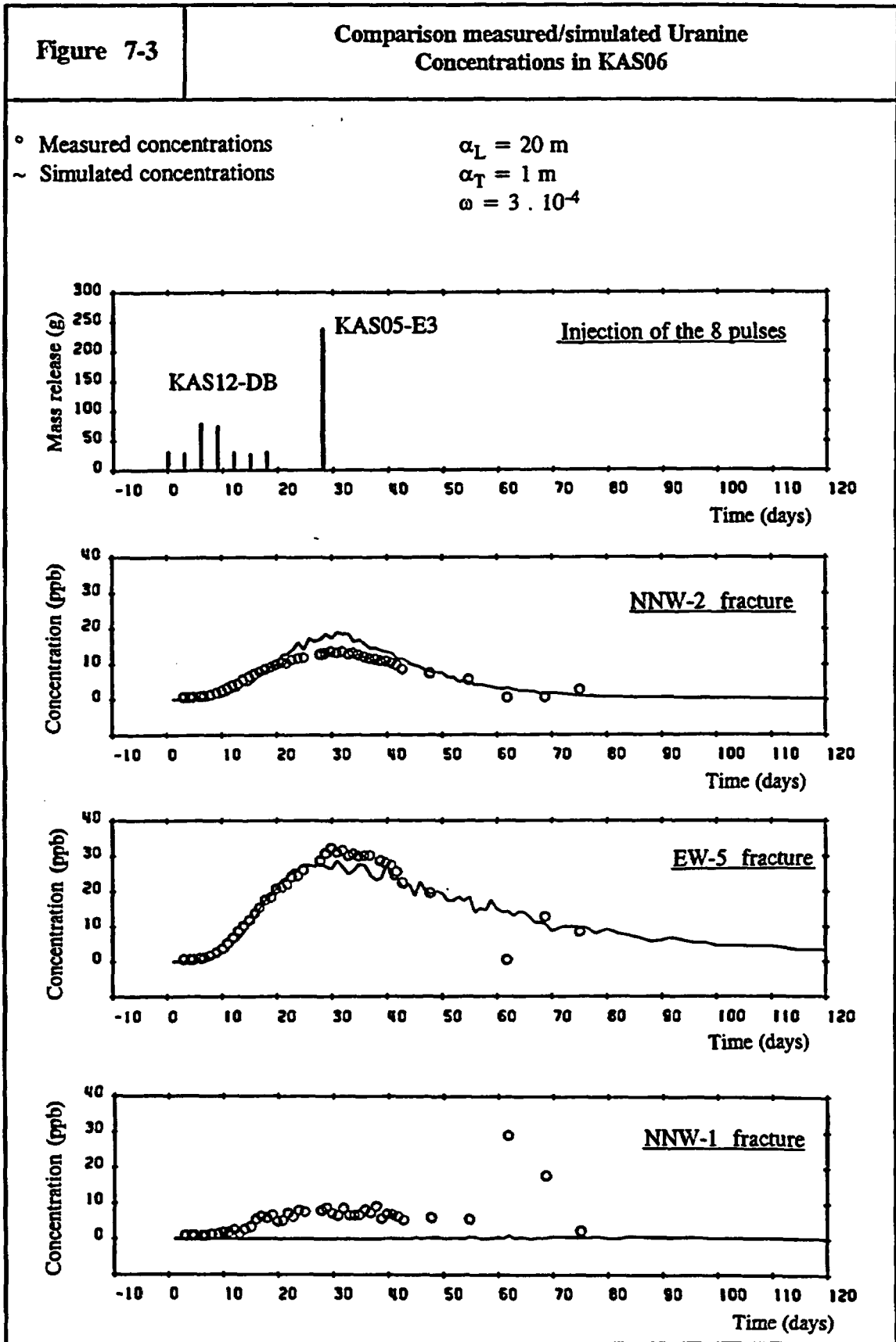
7.3

CONCLUSIONS OF THE TRACER TESTS SIMULATIONS

There seems to be a good coherence of α_L and α_T parameters obtained from these two interpretations ($\alpha_L = 20$ m, $\alpha_T = 1$ to 3 m). It can be noticed that the longitudinal dispersivity is in the order of one tenth of the flow path distance. The contrast observed on kinematic porosities ($9 \cdot 10^{-5}$ to $30 \cdot 10^{-5}$) can be explained by the various paths followed by tracers between the injections sections and the pumping well.

Nevertheless, there is a problem regarding the intersection of the borehole KAS06 with the fracture NNW-1, where simulations give almost no tracer while measures show effective breakthrough curves. This might be an indication of a local problem on connection between fractures, or on kinematic porosity in NNW-1. The hypothesis of insufficient hydraulic connection would be corroborated by the problems encountered during the hydraulic modelling stage, in sections KAS07-J6, DAS13-EE, HAS05-L2 and HAS17-Z2 intersected by fracture NNW-1, where calculated drawdowns were greatly underestimated. As for the transient stage modelling, one or several EW-X fractures added in the conceptual model should increase hydraulic connections, and possibly improve the tracers simulation concerning NNW-1.

The short duration of concentration measurements might be a right explanation of the poor recovery ratios (28%-30%) of Uranine and Rhenium. Especially, it appears that the eighth pulse of Rhenium should have arrived later, after the observation period. Regarding Uranine, the low ratio might be due to delayed breakthroughs in two of the four conductor levels of EW-5 fracture, as well as very slow concentration decrease.



8. GENERAL CONCLUSIONS

In order to model the hydrodynamic context of Äspö Island, a numerical model was created with MARTHE, using the conceptual model developed by SKB.

An adjustment of model parameters for steady state conditions (permeability of matrix, transmissivity of fractures, infiltration) was done in order to more realistically simulate a piezometric map of the natural state and the salinity values measured in wells; it reveals a quality of reconstruction which is satisfactory.

Taking into account the long term pumping test LPT2 does not fundamentally contradict the conceptual model nor the parameters obtained from the analysis of steady state conditions, with the exception of some fractures such as NE-1 and EW-3. It confirms, nevertheless the need to artificially extend the boundaries of the domain by decreasing transmissivities at the intersection of the fractures with the lateral and upper boundaries of the domain. Comparison of calculated and measured drawdowns are generally correct, even if significant differences remain (sections intersected by NNW-1, in particular).

The modelling of tracer experiments carried out during pumping test LPT2 confirms the fact that the conceptual model is a valid approximation. With estimates of the hydrodynamic parameters made during previous calibration stages, the Breakthrough Curves are quite well simulated with a good coherence of hydrodispersive parameters α_L (20 m) and α_T (1-3 m). The differences obtained for the estimation of porosity ($3 \cdot 10^{-4}$ and $9 \cdot 10^{-5}$), attributed globally to the matrix and to fractures all over the domain, are logically justifiable because the corresponding flow paths taken between different injection sections and the pumping well concern different fractures .

A simulation of the pumping test LPT1 shows a large general under-estimation of drawdowns, even if this conclusion can be moderated considering the various problems encountered during this test (in particular, a lack of precision on pressure measurements between packers).

The model obtained after these simulations is therefore reasonably realistic, but with the uncertainties mentioned above. Probably, a large part of these uncertainties should be cleared by simulating the effect of the gallery and the underground laboratory; it would then be necessary to extend the studied domain because the influence of the perturbation is then of an other order of magnitude.

APPENDIX

MODELS AND CODES SPECIFICATIONS

1 NAME, VERSION AND ORIGIN OF THE CODES

Groundwater flow model: MARTHE, version 5.1-1
 Transport model: SESAME, version 3.0
 These two codes have been totally developed by BRGM

2 GENERAL DESCRIPTION

MARTHE is a finite difference code which computes flow rates and hydraulic heads or pressures, for steady and transient states in 2D, 3D or multilayered aquifers. MARTHE includes the computation of density flow and unsaturated zone, as well as automatic calibration features, possibility of multigridding (local nested grid of finer discretization), and modelling of conductive fractures plans intersecting a low permeability matrix.

SESAME is a 3D hydrodispersive numerical model, using a Random Walk particle tracking method, developed to simulate the migration of dissolved substances in groundwater systems. SESAME uses the flow field computed by MARTHE (hydraulic heads or fluxes distribution) to compute the velocities distribution and the transport phenomenons.

MARTHE and SESAME include graphic pre- and post-processing.

3 CONCEPTUAL AND MATHEMATICAL MODEL

MARTHE is a finite difference code with parallelepipedic cells of variable sizes and possibility of nested grids. Density flows are computed by iterative coupling of flow calculation and salinity transport calculation.

In order to compute the groundwater flow in fractured rock, the algorithm described by U. SVENSSON (1990) was included in MARTHE. It consists in determining by means of a geometric calculation the intersections of fractures with the faces of each cell, then computing the exchange coefficients between cells, superimposing fracture transmissivities over matrix permeabilities. Calculation of the intersections of each fracture with each cell boundary allows a precise evaluation of the exchange coefficients between cells, taking into account the real dip of the fractures.

A free surface may locally develop in any layer of the model when $H < z$ (top of the layer), and locally the aquifer may be dried out by pumping or depletion of the water table in deeper layers.

Geographic coordinates are assigned to all the cells in order to allow a precise location of the results.

4 NUMERICAL METHODS

MARTHE includes three solvers: (i) Gauss-Seidel iteration node by node, (ii) iterative scheme by bands (ADI), and (iii) direct solution by conjugate gradients with incomplete Cholesky or Polynomial preconditionning.

MARTHE includes also an algorithm for the identification of parameters by minimizing the differences between measures and model, and for the study of sensitivity to parameters.

In SESAME, the transport of a mass particle is defined by the local flow velocity for convection (Pollock method) and by a random walk draw for dispersion. The main options are: steady/unsteady state flows, instantaneous/continuous injections of a mass from one/several points, delay factor, exponential decay.

5 LIMITATIONS

Up to now hydraulic and transport calculations were not coupled as two separate codes (MARTHE and SESAME) were used. This stage is ending as the Random Walk particle tracking method is being integrated in MARTHE.

6 PARAMETERS REQUIRED

For hydrodynamic calculations, the data required are the following: top and bottom elevation of each aquifer/aquitard mesh, hydraulic conductivities, specific/unconfined storage coefficients, boundary conditions (hydraulic head/density/flux), recharge/discharge fluxes. All these data can be defined by cells or by zones of homogeneous values.

For transport modelling, additional data are required: longitudinal and transversal dispersivity, kinematic porosity, delay factor, exponential decay.

7 TYPE OF RESULTS

Results of computation are given in files, tables, graphs and maps such as spatial distribution/evolution vs time of head/pressure/density/concentration. To allow a complete control of the convergence, additional results such as flow/mass/density balances are given at each time step.

8 COMPUTER REQUIREMENTS

MARTHE and SESAME run either on PC computers (up to 20 000 cells) or on Work Stations (more than 100 000 cells). The codes are the same in both configurations.

9 USER INTERFACE

MARTHE is an integrated code which includes in the same menu all the options required for data analysis, flow simulation, and presentation of results.

SESAME is composed of different submodules to realize these main functions.

10 CODE AVAILABILITY

MARTHE and SESAME can be purchased in BRGM ORLEANS.

11 REFERENCES

Technical description:

- ♦ "Logiciel MARTHE - Modélisation d'Aquifère par un maillage Rectangulaire en régime Transitoire pour le calcul Hydrodynamique des Ecoulements - Version 4.3" - D. THIERY - BRGM Report R 32210
- ♦ "Logiciel SESAME-3D- Modélisation de la migration des pollutions dans les eaux souterraines - Version 2.1-" J.J. SEGUIN, M.L. NOYER, J. SCHWARTZ - ANTEA report A00532

Verification:

- ♦ "Batterie de tests des logiciels de modélisation MARTHE et SESAME" - J.C. MARTIN, Y. BARTHELEMY - BRGM Report R 34797

Application:

More than 80 groundwater flow models using MARTHE during the last 15 years, mainly for groundwater management or waste disposal studies, in 2D, 3D or multilayered aquifers.

About 15 transport models with SESAME.

MARTHE model:

- ♦ "Centre de stockage de la Manche - Modélisation des transports phase 3 tâche 5 - Modèle hydrodynamique phase 5 - Rapport de synthèse" A. GUTIERREZ, P. KASSEM - BRGM Report 610 RP ANT 94-033.
- ♦ "Granite des Deux-Sèvres - Modélisation régionale des écoulements souterrains - Analyse de l'influence des paramètres du modèle sur les flux et les trajectoires". J. SCHWARTZ. BRGM Report 622 RP BRG 91-001
- ♦ "Bassin de Paris - Modèle numérique des formations étagées du Trias au Crétacé supérieur pour l'approche des mécanismes hydrogéologiques". P. ANDRE, Y. BARTHELEMY, D. THIERY - BRGM Report 86 SGN 543 EAU

...

SESAME model:

- ♦ "Etude du système multicouche de la plaine du Tadla (Maroc). Mission 2 : Modélisation numérique pour la gestion des ressources eau eau". Y. BARTHELEMY, P. GOMBERT, J.L. LAVALADE - BRGM Report R 36300
- ♦ "Etude des transferts de pollution sur le site de la COGEMA à Pierrelatte (26)- Rapport de synthèse" - P. CROCHET - BRGM Report R 36168

- ♦ "Nappe alluviale de Marcoule - Etude des transferts en aquifère - Modélisation et applications à MAR600". J.P. SAUTY, J.J. SEGUIN, M. VANDENBEUSCH - BRGM Report R 19120
- ♦ "Participation au test INTRAVAL FINNSJON - Interprétation des tests de traçage en milieu granitique - Modélisation du test de traçage en radial-convergent" -J. SCHWARTZ- BRGM Report 663 RP BRG 93-014

...

List of International Cooperation Reports

ICR 93-01

**Flowmeter measurement in
borehole KAS 16**

P Rouhiainen

June 1993

Supported by TVO, Finland

ICR 93-02

**Development of ROCK-CAD model
for Äspö Hard Rock Laboratory site**

Pauli Saksa, Juha Lindh,

Eero Heikkinen

Fintact KY, Helsinki, Finland

December 1993

Supported by TVO, Finland

ICR 93-03

**Scoping calculations for the Matrix
Diffusion Experiment**

Lars Birgersson¹, Hans Widén¹,
Thomas Ågren¹, Ivars Neretnieks²,
Luis Moreno²

1 Kemakta Konsult AB, Stockholm,
Sweden

2 Royal Institute of Technology,
Stockholm, Sweden

November 1993

Supported by SKB, Sweden

ICR 93-04

**Scoping calculations for the Multiple
Well Tracer Experiment - efficient design
for identifying transport processes**

Rune Nordqvist, Erik Gustafsson,
Peter Andersson

Geosigma AB, Uppsala, Sweden

December 1993

Supported by SKB, Sweden

ICR 94-01

**Scoping calculations for the Multiple
Well Tracer Experiment using a variable
aperture model**

Luis Moreno, Ivars Neretnieks
Department of Chemical Engineering
and Technology, Royal Institute of
Technology, Stockholm, Sweden

January 1994

Supported by SKB, Sweden

ICR 94-02

**Äspö Hard Rock Laboratory. Test plan for
ZEDEX - Zone of Excavation Disturbance
EXperiment. Release 1.0**

February 1994

Supported by ANDRA, NIREX, SKB

ICR 94-03

**The Multiple Well Tracer Experiment -
Scoping calculations**

Urban Svensson

Computer-Aided Fluid Engineering

March 1994

Supported by SKB, Sweden

ICR 94-04

**Design constraints and process discrimination
for the Detailed Scale Tracer Experiments at Äspö -
Multiple Well Tracer Experiment and Matrix Diffusion
Experiment**

Jan-Olof Selroos¹, Anders Winberg²,
Vladimir Cvetkovic²

1 Water Resources Eng., KTH

2 Conterra AB

April 1994

Supported by SKB, Sweden

ICR 94-05

Analysis of LPT2 using the Channel Network model

Björn Gylling¹, Luis Moreno¹,

Ivars Neretnieks¹, Lars Birgersson²

1 Department of Chemical Engineering
and Technology, Royal Institute
of Technology, Stockholm, Sweden

2 Kemakta Konsult AB, Stockholm, Sweden

April 1994

Supported by SKB, Sweden

ICR 94-06

SKB/DOE Hard Rock Laboratory Studies

**Task 3. Geochemical investigations using stable and
radiogenic isotopic methods**

Bill Wallin¹, Zell Peterman²

1 Geokema AB, Lidingö, Sweden

2 U.S. Geological Survey, Denver, Colorado, USA

January 1994

Supported by SKB and U.S.DOE

ICR 94-07

Analyses of LPT2 in the Äspö HRL with continuous anisotropic heterogeneous model

Akira Kobayashi¹, Ryo Yamashita², Masakazu Chijimatsu², Hiroyuki Nishiyama³, Yuzo Ohnishi³

1 Iwate University, Iwate, Japan

2 Hazama Corporation, Ibaraki, Japan

3 Kyoto University, Kyoto, Japan

September 1994

Supported by PNC, Japan

ICR 94-08

Application of three-dimensional smeared fracture model to the groundwater flow and the solute migration of LPT-2 experiment

T Igarashi, Y Tanaka, M Kawanishi

Abiko Research Laboratory, Central Research Institute of Electric Power Industry, Abiko, Japan

October 1994

Supported by CRIEPI, Japan

ICR 94-09

Discrete-fracture modelling of the Äspö LPT-2, large-scale pumping and tracer test

Masahiro Uchida¹, Thomas Doe², William Dershowitz², Andrew Thomas², Peter Wallmann², Atsushi Sawada¹

1 Power Reactor and Nuclear Fuel Development Co., Tokai, Japan

2 Golder Associates Inc., Seattle, WA, USA

March 1994

Supported by PNC, Japan

ICR 94-10

**Äspö Hard Rock Laboratory
International workshop on the use of
tunnel boring machines for deep repositories
Äspö, June 13-14 1994**

Göran Bäckblom (ed.)

Swedish Nuclear Fuel and Waste Management Co.

October 1994

Supported by SKB, Sweden

ICR 94-11

Data analysis and modelling of the LPT2 Pumping and Tracer Transport Test at Äspö. Tracer experiment

Aimo Hautajärvi

VTT Energy

November 1994

Supported by TVO, Finland

ICR 94-12

Modelling the LPT2 Pumping and Tracer Test at Äspö.

Pumping test

Veikko Taivassalo, Lasse Koskinen,
Mikko Laitinen, Jari Löfman, Ferenc Mészáros
VTT Energy
November 1994
Supported by TVO, Finland

ICR 94-13

**Proceedings of The Äspö International Geochemistry
Workshop, June 2-3, 1994, Äspö Hard Rock Laboratory**

Peter Wikberg (chairman), Steven Banwart (proc. ed.)
December 1994
Supported by SKB, TVO, Nirex, ANDRA, CRIEPI

ICR 94-14

Hydrodynamic modelling of the Äspö HRL.

Discrete fracture model

D Billaux¹, F Guérin², J Wendling²
1 ITASCA
2 ANTEA
November 1994
Supported by ANDRA, France

ICR 94-15

Hydrodynamic modelling of the Äspö Hard Rock Laboratory.

ROCKFLOW code

M L Noyer, E Fillion
ANTEA
December 1994
Supported by ANDRA, France